Electrical Properties of Adult Mammalian Motoneurons

Calvin C. Smith and Robert M. Brownstone

Abstract Motoneurons are the 'final common path' between the central nervous system (that intends, selects, commands, and organises movement) and muscles (that produce the behaviour). Motoneurons are not passive relays, but rather integrate synaptic activity to appropriately tune output (spike trains) and therefore the production of muscle force. In this chapter, we focus on studies of mammalian motoneurons, describing their heterogeneity whilst providing a brief historical account of motoneuron recording techniques. Next, we describe adult motoneurons in terms of their passive, transition, and active (repetitive firing) properties. We then discuss modulation of these properties by somatic (C-boutons) and dendritic (persistent inward currents) mechanisms. Finally, we briefly describe select studies of human motor unit physiology and relate them to findings from animal preparations discussed earlier in the chapter. This interphyletic approach to the study of motoneuron physiology is crucial to progress understanding of how these diverse neurons translate intention into behaviour.

Keywords Repetitive firing · Spike frequency adaptation · C-boutons · Persistent inward currents · Modulation

1 Introduction

The primary role of a pool of motoneurons is to work in concert to effect muscle contraction. To do so, each motoneuron of the pool involved in the behaviour must fire trains of action potentials at frequencies that cause its innervated muscle fibres

This chapter is dedicated to two friends who both lost their lives in April, 2019, Doug Stuart and Tom Jessell. Our knowledge of motoneurons would not be where it is today without their relentless quests to understand these fascinating neurons.

C. C. Smith · R. M. Brownstone (✉)
Department of Neuromuscular Diseases, University College London, London, UK
e-mail: calvin.smith@ucl.ac.uk; r.brownstone@ucl.ac.uk

M. J. O'Donovan, M. Falgairolle (eds.), *Vertebrate Motoneurons*, Advances in Neurobiology 28, https://doi.org/10.1007/978-3-031-07167-6_9

to contract with the required force. To do this, a motoneuron integrates inputs from spinal premotor neurons (in some cases including other motoneurons), brain stem, and forebrain, as well as proprioceptive afferents. These inputs inform the motoneuron's output (spike train), and are comprised of excitatory, inhibitory, and modulatory types. Thus to understand how motor commands are transduced into behaviour, it is necessary to understand how motoneurons integrate these various inputs.

Motoneuron integrative properties have primarily been studied using electrophysiological techniques in which glass micropipettes are used to obtain access to the interior of the cell soma by either impalement (sharp microelectrodes) or negative pressure following membrane seal formation (whole cell patch). Electrical responses can be classified into passive (e.g. whole cell capacitance, input resistance), transition (e.g. rheobase, single action potential characteristics), and repetitive firing properties, and are influenced by many factors. One important factor in integration is geometry. Although variable between cells, motoneurons can be large, with inputs arriving at dendrites that extend over millimetres in larger mammals (Fig. 1). The location of these inputs relative to the integrative site at the axon initial segment influences their "value" in the production of spike trains.

A motoneuron is defined by its output: these are neurons that innervate muscle fibres. (While there are indeed other post-synaptic targets, a key role is to cause muscle contraction; other targets are considered in other chapters.) Somatic motoneurons, to be considered here, innervate skeletal muscle fibres. While this may seem to be a sufficiently restricted definition, there is great diversity within motoneurons within any given animal. That is, there are many subgroups of motoneurons

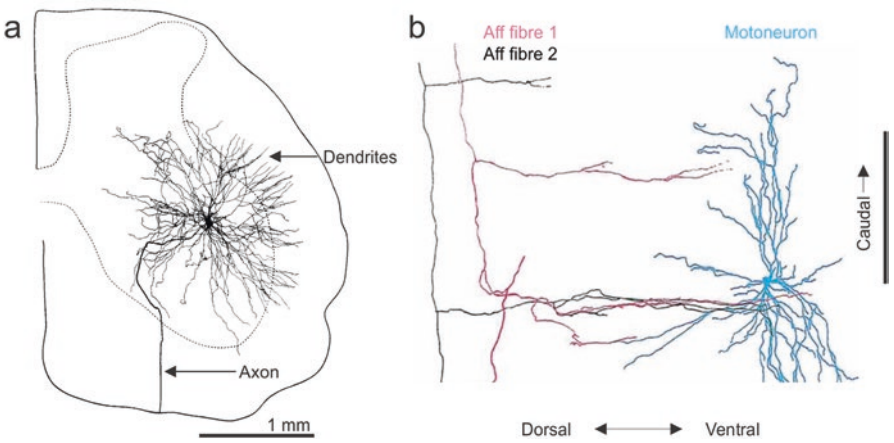

Fig. 1 Anatomy of a motoneuron. (**a**) Intracellularly filled, 3D reconstructed, adult cat triceps surae motoneuron shown in a transverse section of the lumbar spinal cord. *Arrows* show axon (no tapering) and dendritic field, which can extend more that 1 mm from the soma. (**b**) Intracellularly filled, 3D reconstructed, medial gastrocnemius motoneurons (blue) and invading proprioceptive afferent fibres (*Aff,* pink and black). Longitudinal/oblique spinal cord slice. Both scale bars are 1 mm. (**a**) from Ulfhake et al. (1988), Fig. 5d. (**b**) from Burke and Glenn (1996), Fig. 1

within both the brain stem and spinal cord, and these subgroups have different integrative properties.

Somatic motoneurons in the brain stem include those that innervate the extraocular muscles (Evinger 1988), the muscles of mastication (Yamada et al. 2005), of the face (including whisking motoneurons in some species; Kleinfeld et al. 2014), of the oropharynx (Gestreau et al. 2005), of the larynx, and the tongue. Some of these populations have been studied more thoroughly than others, but it is clear that their properties differ from each other. Oculomotor neurons, for example, can fire at rates of up to 400 Hz (Tsuzuki et al. 1995), far faster than trigeminal motoneurons (Chandler et al. 1994), for example.

Motoneurons are located throughout the spinal cord, where they organise into columns during development. The phrenic motor column is in cervical C3–5 segments and innervates the diaphragm. In the cervical and lumbar spinal cord, medial motor column (MMC) motoneurons innervate epaxial (including, for example, erector spinae, multifidus, semispinalis, and splenius) muscle fibres (Tsuchida et al. 1994), and the lateral motor column (LMC) motoneurons are limb-innervating. Motoneurons innervating external urethral and anal sphincter muscles, and those innervating tail muscles are in the sacral spinal cord. LMC motoneurons have been most extensively studied and thus form the basis of much of our knowledge of motoneuron properties.

The LMC itself can be divided into columns (medial (LMC_m) and lateral (LMC_l)), which in turn can be subdivided into columels that contain motor pools (for review see, Stifani 2014). A motor pool is a population of motoneurons that innervates a single muscle (Kanning et al. 2010). There is further granularity within motor pools themselves, as most are comprised of motoneurons with different functions. γ-motoneurons, which are about 30% of many pools, innervate the contractile components of the sensory organs of muscles, muscle spindles (Granit 1975), whereas α-motoneurons innervate extrafusal fibres responsible for force production. In addition, β-motoneurons innervate both spindles and extrafusal fibres. α-motoneurons within a pool can be further sub-divided based on the muscle fibre type they innervate (type I, or slow twitch, type IIa or fast twitch fatigue-resistant, type IIb and IIx, fast twitch fatigable). An α-motoneuron and the muscle fibres it innervates are together called a motor unit (Liddell and Sherrington 1924). These motoneurons have electrophysiological properties that correspond to the fibre types they innervate, and are termed S, FR, and FF (slow, fast fatigue resistant, and fast fatigable) motoneurons (Burke et al. 1973).

Given their diversity, it is no wonder that motoneurons have diverse electrophysiological properties and it is thus impossible to define these properties for an "idealised" motoneuron. In this chapter, we will present a brief history of motoneuron recordings from Lord Adrian to the present day, and then discuss passive, transition, and repetitive firing properties, focusing on the properties and subtypes of spinal LMC α-motoneurons. We also discuss motoneuron modulation by somatic (C-boutons) and dendritic (persistent inward currents) pathways, and finally, human studies of motor unit physiology.

Foundational Studies of Motoneuron Properties

While Sherrington studied motor output from the behavioural viewpoint, it was Lord Adrian who first recorded mammalian motor axons (Adrian and Bronk 1929). These experiments revealed repetitive spike trains from phrenic motor nerves at frequencies which seemingly covaried with the contraction force. Eccles and Hoff (1932) followed this up with a study in which they modified these spike trains using electrical stimulation, leading them to propose that the neurons of origin had a "central excitatory state" that was depressed after each spike. They further concluded that these depressions could summate – this turned out to be prescient of the phenomenon of the summation of post-spike afterhyperpolarisations described by Ito and Oshima (1962).

With the advent of the paraphernalia required for intracellular recording that followed on studies of invertebrate neuronal excitability (Hodgkin and Huxley 1939), two groups began to record cat motoneurons in anaesthetised preparations (Brock et al. 1951; Brownstone 2006 review for a full account). These seminal studies led to an understanding of the basic electrical properties of motoneurons, which were then formalised by Rall and co-workers (Rall 1960; Eccles 1961). Meanwhile, Kernell and colleagues outlined repetitive firing properties, defining the relationships between motoneuron input and output (Granit et al. 1966a, b). Thus, by the end of the 1960s, we had a good understanding of the fundamental passive, transition, and repetitive firing properties of motoneurons.

All of the above experiments were done in vivo, mostly in anaesthetised preparations although some in decerebrate preparations. It became evident that motoneuron properties are "state-dependent" – i.e. different if recorded under anaesthesia vs in the decerebrate preparation, and different during induced locomotor activity than at rest (Brownstone et al. 1992). Most of these early experiments were in cat (with a few in rats), and all were done with sharp electrodes, "blindly" seeking ventral horn neurons that could be identified by their antidromic responses to stimulation of muscle nerves. All were in motoneurons innervating the hindlimb (usually left), and most innervated extensor muscles such as gastrocnemius. And because they were done with sharp electrodes, the probability was in favour of recording the largest motoneurons (type F), although some studies intentionally sampled a wide range (Zengel et al. 1985). In other words, much of our early knowledge of motoneuron electrophysiological properties has been derived from a rather limited selection of these diverse neurons.

The advent of slice preparations and patch clamping led to the study of membrane channels responsible for neuronal properties (Edwards et al. 1989; Dodt and Zieglgänsberger 1990; Sakmann and Neher 1984), which in turn led to the use of spinal cord slice preparations to study motoneuron properties (Takahashi 1978; Konishi and Otsuka 1974). Unfortunately, these studies have largely been confined to neonatal MNs, neurons that have properties that are still under development during their critical period.

2 Passive Properties of Motoneurons and Elementary Cable Theory

As the "final common path" that functions to cause effective muscle contraction, the ultimate goal of a motoneuron is to fire trains of action potentials in response to synaptic inputs to its soma and extensive dendritic tree. These inputs must be integrated to provide sustained depolarisation that is sufficient to initiate repetitive firing at a particular rate. In this section, we will look at the basic factors that govern this integration, which are the passive electrical properties of motoneurons: input resistance, whole cell capacitance, membrane time constant, and length constant. For a more thorough discussion of these properties and their contribution to integration, the reader is directed to Rall (2011).

The input resistance (R_N) is usually measured by injecting small amounts of current to cause voltage deflections that do not activate voltage-sensitive channels (Fig. 2a), and is calculated using Ohm's law:

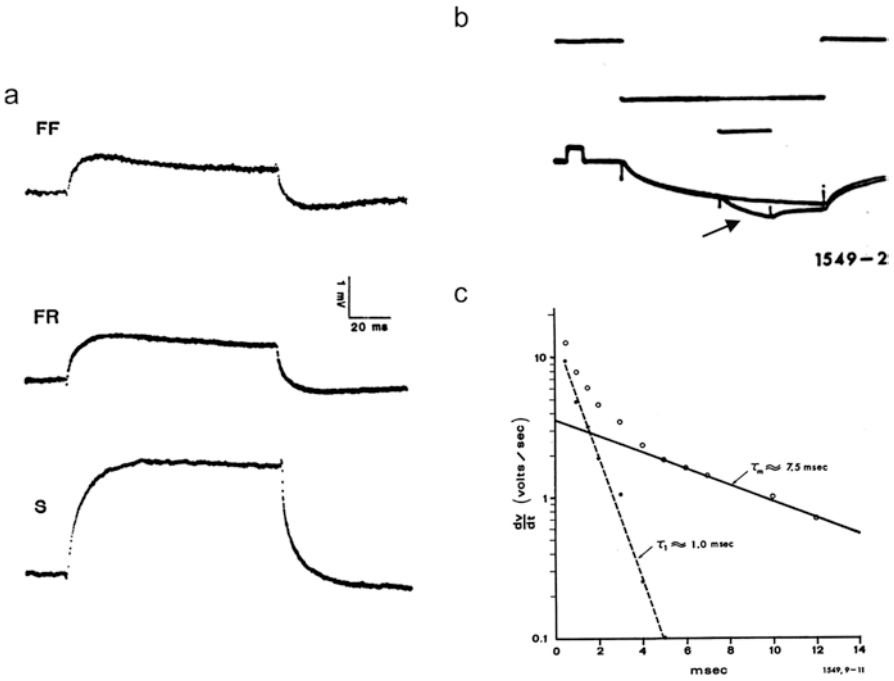

Fig. 2 Passive properties of an adult cat motoneuron. (**a**) Input resistance: Voltage response to current injection in slow (*S*), fast fatigue resistant (*FR*) and fast fatigable (*FF*) medial gastrocnemius motoneurons. (**b**) Time constant: Response recorded intracellularly to hyperpolarising current injection, current in *upper trace*, voltage in *lower trace*. Voltage calibration *pulse* is 10 mV, 1 ms. *Arrow* indicates transient analysed in c. (**c**) Slope vs time of voltage transient in b reveals more than one exponential. By subtracting the long exponential, a second linear component is revealed, showing the data can be approximated by the sum of two exponentials. The ratio of the two time constants is related to the electrotonic length of the dendritic tree. **a** is from Zengel et al. (1985), Fig. 3. (**b** and **c**) from Nelson and Lux (1970), Fig. 5d, 6

$$R_N = V / I \quad (1)$$

where V is the voltage deflection produced by the current (I) injected.

There are several important factors that will impact these measurements:

(a) Leak around the electrode, which is greater for sharp than patch electrodes – this can lead to an order of magnitude difference in measurement (Li et al. 2004a);
(b) "state" during which the measurements are taken, e.g. in vitro vs in vivo, the type of anaesthesia, decerebration (see, for example, Kernell 1999); and
(c) Intactness of the dendritic tree, which will be affected in slice preparations (typically sampled at 300–350 μm thick; Smith and Brownstone 2020), disproportionately affecting larger (e.g. more mature and/or faster) motoneurons. Juvenile mouse motoneuron dendrites can extend at least 0.5–1 mm from the soma (Leroy et al. 2014; Fukuda et al. 2020).

Furthermore, there is a high degree of biological variance between motoneurons, as small (type S) motoneurons have much higher input resistances than large (FF) motoneurons. These differences will also lead to systematic differences in measurements between studies: for example, in vivo studies that "blindly" target motoneurons will tend to bias towards the largest, lowest resistance motoneurons, and slice experiments generally tend to favour the smaller (S) motoneurons as they more readily survive in vitro (Mitra and Brownstone (2012) reported a mean R_N of 123 MΩ for lumbar motoneurons in postnatal day (P)43+ slice preparations, whereas Smith and Brownstone (2020) reported a mean R_N of 31 MΩ at P14–21). Nevertheless, we can make some general statements about input resistance: cat lumbar motoneurons (with sharp electrodes) range from 0.1 to 4 MΩ (Zengel et al. 1985), mouse motoneurons in vivo range from 1 to 12 MΩ (Meehan et al. 2010), and motoneurons from the mature (>P15) mouse lumbar spinal cord in slices (patch recordings) range from 2 to 200 MΩ (Smith and Brownstone 2020; Bhumbra and Beato 2018; Mitra and Brownstone 2012). These differences arise from the factors listed above.

Whole cell capacitance reflects the charge that the neuronal membrane can store, which depends on specific membrane capacity and membrane surface area. Since the former, a property of the lipid bilayer, is the same across all neurons, capacitance measurements reflect the size of the neuron, or the amount of membrane area affected by the current pulse.

Whole cell capacitance (C) is calculated from measurements of membrane time constant, τ and input resistance, R_N:

$$\tau = R_N * C \quad (2)$$

The time constant can be measured by fitting an exponential to the decay of membrane potential following a subthreshold pulse (Fig. 2b, c). The time course of a voltage change depends on τ such that at time t,

$$V = V_0 * e^{-t/\tau} \quad (3)$$

where V_0 is the initial voltage, and assuming that there is perfect space clamp (that is, that voltage is uniform throughout the cell). It can be seen that the time constant represents the time at which the voltage decays by 1/e, or to about 37% of the initial voltage. Typical measurements for capacitance and time constant are, respectively: 1.5 to 15 nF and 3 to 15 ms for cat motoneurons, and 0.2 to 1 nF and 2 to 20 ms for mature mouse motoneurons.

It is important to consider the membrane time constant when examining integration of synaptic inputs: the shorter the time constant, the faster a depolarising potential will rise and decay, thus affecting temporal summation. Temporal summation, or the summation of EPSPs close to each other in time, depends largely on the decay time of the EPSPs as rise times are very fast (see Iansek and Redman 1973a). This decay is more dependent on the time constant of the synaptic conductance and/or the membrane time constant, whichever is greater. Efficient temporal summation requires a frequency of excitatory inputs that at least matches the time constant of EPSP decay. In FF MNs, which have membrane and AMPA receptor time constants in the range of 1–2 ms, proximal unitary EPSPs correspondingly decay rapidly (Burke 1967). This fast τ would thus minimise temporal summation in these neurons, suggesting that close to concurrent excitatory inputs or activation of longer time constant synaptic conductances (such as those mediated by NMDA receptors) are needed for effective summation. But note also that temporal summation at a single location would at best be sublinear: the driving force for the second EPSP would be reduced, and the local conductance would be increased, both effects contributing to sublinear summation.

The basic properties above are, in the first instance, particularly relevant for spherical neurons. But motoneurons have extensive dendritic trees, and thus other factors come into play. Wilfred Rall [1922–2018] applied cable theory to motoneurons in order to put these factors together, so as to understand passive motoneuron properties and how they affect motoneuron integration. The strength of Rall's work on cable theory was its close relationship with experimental neuroscience, each informing the other.

One example of the interaction of theory and experiment arose from the analysis of τ. When measuring τ as above, it can be seen – particularly when very brief current pulses are delivered – that more than one exponential can be fit to the voltage decay (Fig. 2c). This multi-exponential decay results from a lack of space clamp: neurons are not spheres, and the current injected does not lead to a membrane that is isopotential throughout the dendritic tree. That is, there is voltage decay due to current flow both across the membrane and through the cell, along dendritic branches. This latter current flow is dependent on axial resistance, R_i, which in turn depends on cross-sectional area of the process in which the current flows.

The length constant, λ, is an indication of the decay of voltage along the length of dendrite, such that

$$V = V_0 * e^{-x/\lambda} \tag{4}$$

where x is the distance along the dendrite from the voltage change V_0. Thus, a voltage decays to 1/e (~37%) of its value at distance λ. In other words, the larger the length constant, the less decay of the voltage for any given length, and thus the more "effective" that voltage would be at a distance.

The length constant is dependent on the axial resistance and the membrane resistance such that λ can be approximated by:

$$\lambda = \left(r_m / r_i\right)^{1/2} \tag{5}$$

or

$$\lambda = \left[\left(R_m / R_i\right)\left(d / 4\right)\right]^{1/2} \tag{6}$$

where r_m is the resistance across a unit length of membrane (Ω-cm), r_i is the axial resistance per unit length (Ω/cm), R_m is the membrane resistivity (resistance across a unit area of membrane, Ω-cm^2), R_i is the intracellular resistivity (Ω/cm), and d is the diameter of the dendrite (cm).

While it is thus difficult to measure λ, it is possible to measure its consequences. That is, the dendritic tree can be thought of in terms of its electrotonic length, L, or the length of a dendrite (ℓ) in terms of the number of length constants:

$$L = \ell / \lambda \tag{7}$$

L can be estimated by measuring the time constant of current spread within the neuron. By injecting a brief current pulse, two time constants can be peeled from the voltage decay (Nelson and Lux 1970; Rall 1967). The slowest τ (τ_0 or τ_m) would reflect the membrane time constant, and the next slowest, τ_1, and others (τ_2 and theoretically beyond) the time constant of the cable(s), reflecting the equalisation of voltage through the neuron. The ratio of τ_0/τ_1 reflects L. In cat motoneurons, L = 1.0–2.1 (mean 1.5; Iansek and Redman 1973a), indicating that the depolarisation in the soma would be about 22% ($1/e^{1.5}$) of the voltage produced by an excitatory post-synaptic potential (EPSP) at the dendritic tip.

Understanding these principles has proven to be very useful in understanding motoneuron integration. For example, using cable theory and meticulous measurements of cable properties in cat motoneurons, the shapes of EPSPs (rise times and half-widths) can be studied to reveal their location on the dendritic trees and the synaptic currents they produce there (Iansek and Redman 1973b). Doing so revealed that the quantal content of synapses on dendrites are far greater than those on somata.

Thus, in the soma, changes in voltage produced by synaptic inputs throughout the motoneuron are dependent on space and time, and can be expressed by this partial differential equation of cable theory:

$$\lambda^2 \partial^2 V / \partial x^2 - V - \tau \partial V / \partial t = 0 \tag{8}$$

The time constant τ influences temporal summation, and the length constant λ influences spatial summation.

It may seem that cable theory is limited by the underlying assumption that dendritic membranes are passive. However, even so, cable theory is foundational for understanding how active dendrites contribute to motoneuron integration (see below).

3 Motoneuron Transition Properties

Transition properties can be defined to include subthreshold voltage-gated conductances, as well as properties that influence single action potentials. These are the attributes that, while influenced by passive properties, are foundational for the ultimate goal of motoneurons: producing repetitive spike trains.

Sag and Post-inhibitory Rebound

A subthreshold phenomenon that can contribute to motoneuron recruitment is the sag potential. Sag potentials are seen when a rectangular hyperpolarising current is injected to produce a voltage response that after a delay (perhaps ~100 ms; Bayliss et al. 1994) starts to return (rectify) towards resting potential. Upon cessation of the hyperpolarisation, this slow inward current that has been activated causes the membrane voltage to rebound beyond rest, producing post-inhibitory rebound (PIR). The PIR is characterised by 'over-rectification' following inhibitory input, producing a depolarising 'hump'. Voltage clamp studies have shown that conductances mediating sag potentials (I_h) are non-specific cation conductances carried by a family of hyperpolarisation-activated cyclic nucleotide-gated channels (HCN; Zemankovics et al. 2010).

There is evidence that I_h can be modulated by monoaminergic inputs, and thus can contribute to motoneuron activity in a state-dependent manner (Takahashi and Berger 1990; Larkman and Kelly 1992). Activation of I_h during the hyperpolarised phase of the locomotor cycle may also contribute to PIR-induced firing to assist in initiating the active phase of the step cycle (Bertrand and Cazalets 1998; Hochman et al. 1994). Of note, as well as HCN-mediated I_h, a calcium current carried by low voltage-activated Ca^{2+} (Ca_V3) channels can contribute to PIR (Canto-Bustos et al. 2014).

Rheobase

When depolarisation of the axon initial segment is sufficient such that it reaches threshold, an action potential is initiated. The minimum current needed for this to occur, rheobase, depends on the passive properties of the motoneuron (see above),

in particular R_N. Thus, smaller S-type motoneurons with higher R_N have lower rheobase currents than the larger, lower R_N FR and FF motoneurons.

In 1957, Henneman described the "size principle," in which motoneurons are recruited by synaptic inputs in order from the smallest to the largest size (Henneman 1957). This "orderly recruitment" of motoneurons in response to stimulation of spindle primary afferents fits with the distribution of rheobase currents across different motoneuron types. That is, given that each primary afferent projects to every motoneuron in its pool (at least in the adult cat; Baldissera et al. 1981), then if synaptic transmission at the fibre terminals produces approximately an equivalent synaptic current, higher currents (produced by increasing stimulation) would be necessary to recruit the higher rheobase, larger motoneurons. These neurons would thereby only be recruited in response to afferent activity greater than would activate the lower rheobase, smaller motoneurons.

Action Potential Characteristics

Changes to spike frequency and spike timing are influenced by changes in motoneuron action potential morphology (Fig. 3a). As all-or-none phenomena, action potentials, regardless of neuron type, have the same phases: threshold, depolarisation (rising), repolarisation (falling), fast after hyperpolarisation (fAHP), after depolarisation (ADP), and medium after hyperpolarisation (mAHP, Fig. 3a). However, due to the relative expression of constitutive ion channels, the duration and/or amplitude of these phases varies between neurons.

Threshold and Rising Phase

The voltage threshold is the voltage at which an action potential is generated; this voltage can change over time and with behaviour. When the membrane potential reaches threshold, voltage-gated sodium channels are activated, initiating a rapid depolarisation of the membrane potential constituting the rising phase of the spike, which usually results in an overshoot greater than 0 mV (Barrett and Crill 1980). Given the reliance of the spike on sodium channel availability, an increase in the proportion of inactivated channels will depolarise the voltage threshold. Therefore, the voltage threshold in response to slow depolarisations is less negative than following rapid depolarisations.

Initial assessments of motoneuron action potentials were done in cats and described 2 distinct 'spike potentials: an 'A' and a 'B' spike (Brock et al. 1951; Fuortes et al. 1957). The small spike is an initial depolarisation to an inflection point followed by a rapid depolarisation to peak. An elegant set of experiments by Coombs et al. (1957) showed that the size of the A and B spikes change relative to the position of the microelectrode between the soma-dendritic (SD) compartment and the axon initial segment (IS). When the electrode penetrates close to the initial axon

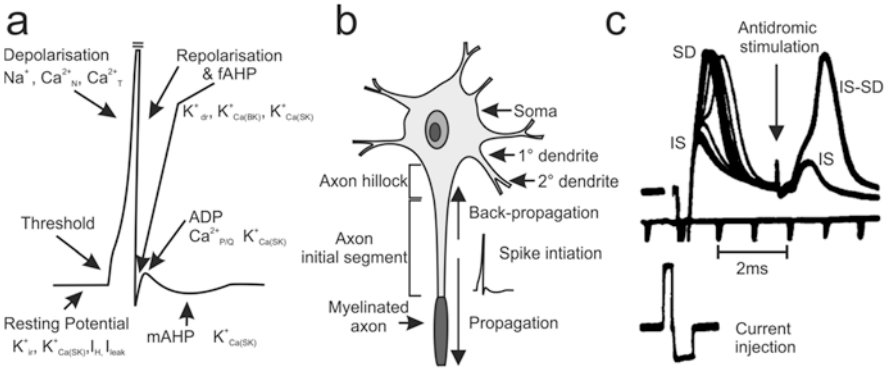

Fig. 3 Motoneuron action potential characteristics and generation. (**a**) Each phase of the action potential identified by *arrows* with a sampling of associated conductances indicated. (**b**) Schematic illustrating motoneuron proximal morphology and highlighting the axon initial segment, where spikes are generated. (**c**) Traces showing initial segment (IS) and somato-dendritic (SD) spikes. The top trace is the membrane potential and shows several large and small spikes evoked by either intracellular current injection (bottom trace, after 1 ms) or antidromic activation via peripheral nerve stimulation (artefact on top trace, after ~3.7 ms). Depolarising current pulses evoked high amplitude spikes, which represent *SD* spikes. When depolarising pulses are followed by a brief hyperpolarising pulse, the *SD* spike is inhibited and reveals the *IS* spike. When "intermediate sized" hyperpolarising pulses at threshold for suppression preceded antidromic stimulation, either *IS* or *IS-SD* spikes were evoked. (**a**) was adapted from Nordstrom et al. (2007), Fig. 1. (**b**) is from Li et al. (2004b), Fig. 2b, and (**c**) is from Coombs et al. (1957), Fig. 11f

segment (Fig. 3b), the A spike is larger than the B spike, whereas if well into the soma, the B spike is larger. Ultimately, this led to the adoption of the more specific nomenclature, with the early phase called the IS spike and the later the SD spike (Fig. 3c). Because the IS spike has a lower threshold and precedes the SD, it was concluded that action potentials are initiated in the axon IS.

The high excitability of the initial segment is due to the differential expression of ion channels, acquired during early embryogenesis (Le Bras et al. 2014). The boundaries of the IS are clearly defined by expression of the scaffolding protein ankyrin G (AnkG), which is crucial for assembly of the IS. The motoneuron IS expresses 2 main sodium channels, $Na_V1.6$ which is expressed throughout the IS, and Na_V 1.1 expressed at the axon hillock (Duflocq et al. 2008, 2011). A variety of potassium channels ($K_V7.2$, $K_V1.1$, $K_V1.2$ and $K_V\beta2$) are also expressed in the IS, ensuring a fast repolarisation of the membrane potential at this site (Garrido et al. 2003; Pan et al. 2006; Lorincz and Nusser 2008).

While many factors influence threshold, motoneuron type does not. Although threshold varies between motoneurons, there is no systematic difference in voltage threshold between fast and slow motoneurons, or between those from cervical and lumbar cord (Pinter et al. 1983; Smith and Brownstone 2020). Thus it is unlikely that threshold contributes to orderly recruitment of the size principle (Henneman 1957).

There is evidence that the voltage threshold of motoneurons is state-dependent, and thus likely subject to neuromodulatory control. During fictive locomotion in the cat, voltage threshold is hyperpolarised in relation to the control threshold (Krawitz et al. 2001). Therefore, modulation of this property is likely another tool available to the nervous system for regulating motor output.

Repolarisation Phase and fAHP

There is a greater diversity of ion channels contributing to the falling compared to the rising phase of the action potential. These include voltage activated delayed rectifier potassium channels, rapidly inactivating potassium channels, and small conductance calcium-dependent potassium (SK) channels (Sah and McLachlan 1992; Schwindt and Crill 1981; Barrett and Barret 1976). Action potentials tend to be wider in slow motoneurons compared to fast (Krutki et al. 2017), suggesting differential expression of the channels involved in the falling phase.

The fast after hyperpolarisation (*f*AHP) marks the end of the action potential and is largely determined by the same currents responsible for the repolarisation phase of the AP. The amplitude and duration of the *f*AHP varies with motoneuron type and species as it is quite prominent in smaller animals such as frogs (Barrett and Barret 1976), toads (Araki and Otani 1955), turtles (Hounsgaard et al. 1988b), and rodents, but less so in the cat. The trough voltage of the fAHP was found to be very constant regardless of how the spike was initiated (Kolmodin and Skoglund 1958), and is thought to represent a high conductance state due to the delayed rectifier potassium conductances (Krnjević et al. 1978; Nelson and Burke 1967).

Afterdepolarisation

Motoneuron action potentials may have a short depolarisation phase immediately following the *f*AHP, called the afterdepolarisation (ADP; Granit et al. 1963b; Kernell 1964). The ADP is thought to be dependent upon voltage-gated Ca^{2+} channels as it can be blocked by cadmium and enhanced by increasing extracellular Ca^{2+} concentrations (Kobayashi et al. 1997).

A prominent ADP can reach threshold and promote high frequency spike doublets or triplets at the start of an action potential train (Spielmann et al. 1993). These "additional" spikes that ride upon the ADP of the initial action potential were described as defining 'the catch property' of motoneurons by Burke et al. (1970). The group showed that while stimulating a motoneuron to produce a spike train, a single extra stimulus with an interval of <10 ms added to the start of the train increased the rate of force generation and induced long lasting enhancement of tension in the innervated muscle. Stein and Parmiggiani (1979) used extracellular stimulation to confirm that high initial frequencies followed by slower spiking is the

most efficient for muscle force generation (Garland and Griffin 1999; Parmiggiani and Stein 1981). Thus, the ADP promotes high initial firing frequencies in motoneuron spike trains, thereby enhancing rate and magnitude of force generation. Interestingly, slow motoneurons tend to express greater amplitude ADPs and are therefore more likely to produce doublets than fast motoneurons (Spielmann et al. 1993).

Medium Afterhyperpolarisation

From the very first intracellular recordings from motoneurons it was noticed that the AHP was responsible for the refractory period and therefore regulated firing frequency (Brock et al. 1951). It is now well established that the medium afterhyperpolarisation (mAHP) amplitude and duration correlate inversely with motoneuron size (Eccles et al. 1958). Slower motoneurons have a larger amplitude, longer duration mAHP compared to fast motoneurons and fire at lower frequencies. The majority of the mAHP current is carried by SK channels, which can be selectively blocked by apamin (Kobayashi et al. 1997; Zhang and Krnjević 1987). As might be expected by the different characteristics of the mAHP in slow vs fast motoneurons, SK channel expression also differs between the 2 types (Deardorff et al. 2013). There are several different SK isoforms, but only SK2 and 3 have been identified in motoneurons to date. SK2 is expressed by all motoneurons, but the expression of SK3 channels is lower or absent in fast motoneurons, and dominates in slow motoneurons (Deardorff et al. 2013). It is thus likely the SK3 channels that are responsible for the larger mAHP.

The source of calcium that leads to SK channel activation is unknown, but several studies have shown that Ca_V2 (N and P/Q type Ca^{2+}) channels are necessary for generation of the mAHP (Li and Bennett 2007; Bayliss et al. 1995; Umemiya and Berger 1994). Given the clustering of SK channels at C-bouton synapses and their proximity to Ca^{2+} stores in the subsurface cisternae (see below), it is possible that local intracellular Ca^{2+} release also contributes to SK channel activation and the mAHP. The mAHP is the target of modulatory inputs to motoneurons, with reductions in the mAHP amplitude/duration leading to significant increases in excitability as determined by the f-I relationship. During locomotor activity, the mAHP is reduced and high frequency firing ensues (Brownstone et al. 1992).

4 Repetitive Firing Properties of Motoneurons

Ultimately, it is the role of a motoneuron to translate synaptic inputs into repetitive spike trains at a frequency appropriate to produce the contraction of its innervated muscle fibres required for a given task. Motoneurons fire action potentials repetitively in response to repetitive (Eccles and Hoff 1932) or sustained input (Barron

and Matthews 1938), with a positive relationship between the frequency of output and the magnitude of current input. This frequency-current (f-I) relationship (Fig. 4a) has been extensively studied to quantify motoneuron excitability using both sustained rectangular current pulses and slow triangular ramps (Fig. 4b).

Between 2 and 4 different 'ranges' of firing have been demarcated, largely in studies of cat motoneurons, by changes in the slope of the f-I curve (Fig. 4a, b). The two main ranges have been designated as the primary and secondary ranges (Granit et al. 1966a, b), with a tertiary range (Schwindt 1973) sometimes seen. In addition, a sub-primary range (Manuel et al. 2009; Jensen et al. 2018), thought to be related to mixed mode membrane oscillations (high frequency, sub-threshold membrane potential oscillations) has also been identified in some conditions in mouse motoneurons (Iglesias et al. 2011; Fig. 4c, d).

Each of the ranges is more-or-less linear. In cat motoneurons, the primary range is characterised by a relatively low f-I slope, with transitions to the secondary range seen by a sharp increase in slope (Granit et al. 1966a, b). A third segment, the tertiary range, is usually demarcated by a sudden reduction in f-I slope (to below that of the primary range), although in some motoneurons it has the steepest slope (Schwindt 1973). In mouse motoneurons, the secondary range, if present, typically has a lower slope than the primary range. Possible mechanisms underlying this transition are discussed below (*Persistent inward currents*).

To understand how different ranges of the f-I relationship relate to force generation in the muscle, it is important to consider the contractile properties of the muscle fibres innervated. Motoneuron firing frequency is tuned to the force output of the muscle fibre innervated, with increases in frequency resulting in repetitive twitch contractions that summate. As firing frequency increases, the twitch contractions fuse until maximum force is generated, at which point further increases in spike frequency are superfluous. This relationship can be seen by the sigmoid shape of the relationship between tension and stimulation frequency (Kernell 1983; Cooper and Eccles 1930).

Contraction properties differ in different muscle fibre types; motoneuron properties are tuned to the muscle fibre types they innervate, and thus their firing frequencies differ. For example, the firing frequency at which maximum tetanic force is produced will differ depending not only on the motor unit assessed, but also the species (smaller animals have faster equivalent motor units). Our understanding of the relationship between motoneuron firing frequency and muscle force production comes mainly from studies in cats (Kernell 2006). However, contemporary studies of motor unit physiology use rodent models, particularly the mouse. The maximum muscle force output in rats, for example, is generally achieved at the start of the primary or early secondary range of motoneuron firing (Turkin et al. 2010), and in anaesthetised mice, there is evidence to suggest that near maximal force can be generated by sub-primary range firing (Manuel and Heckman 2011). It is unclear why, at least in smaller mammals, motoneuron firing ranges exceed the contractile force capabilities of the muscles they innervate.

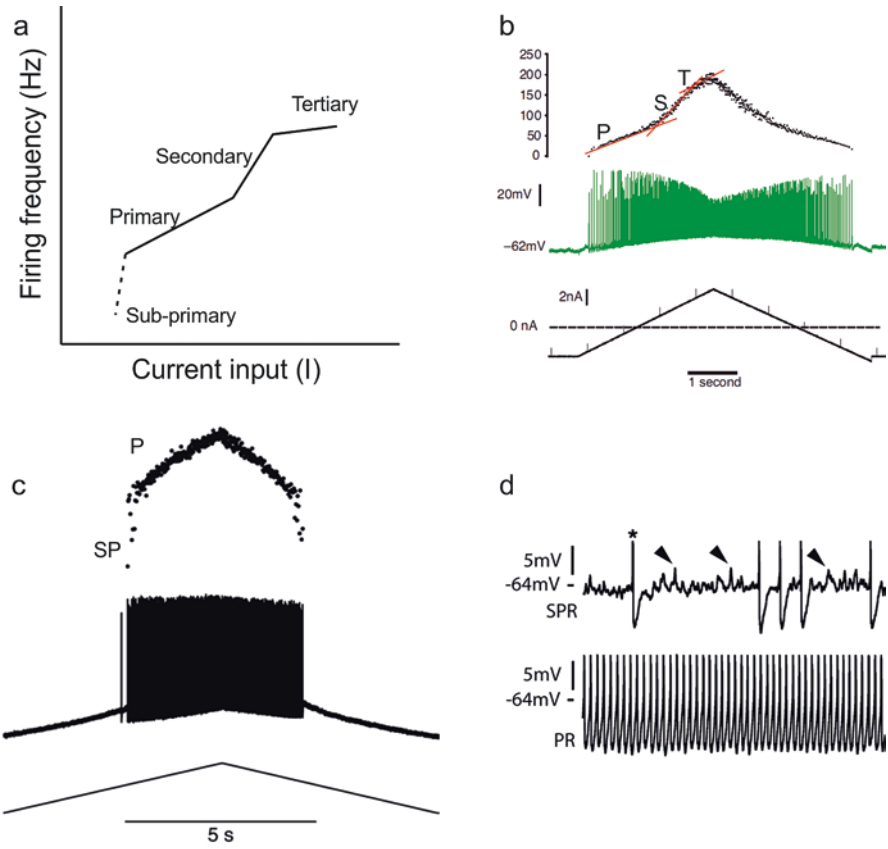

Fig. 4 Repetitive firing patterns in motoneurons. (**a**) Frequency-current plot schematic. The primary, secondary and tertiary ranges (*solid lines*) are labelled and the sub-primary range is the *dashed line*. (**b**) Voltage trace (*middle*) during current clamp experiment in an adult rat motoneuron shows firing in response to a triangular current ramp (*lower trace*). The *top trace* is a plot showing the instantaneous firing frequencies during the primary (P), secondary (S) and tertiary (T) ranges. (**c**) Similar layout as b showing the sub-primary (SP) and primary (P) ranges in an adult mouse motoneuron. (**d**) Irregular adult mouse motoneuron firing produced in sub-primary range due to mixed mode oscillations (*upper trace*). Firing in primary range is regular (*lower trace*). Spikes truncated for illustrative purposes. (**a**) adapted from Heckman et al. (2005), Fig. 1b. (**b**) adapted from Jensen et al. (2020), Fig. 6A. (**c**) from Manuel et al. (2009), Fig. 8b1. (**d**) from Iglesias et al. (2011), Fig. 1b1

Spike Frequency Adaptation

When long supra-threshold rectangular currents are injected into a motoneuron, inter-spike-intervals (ISI) become longer over the duration of the pulse (Fig. 5a). This slowing of instantaneous spike frequency is termed spike frequency adaptation (SFA). There are 2 main phases of spike frequency adaptation. Early SFA represents the slowing of spike frequency over the first hundreds of milliseconds (Granit et al.

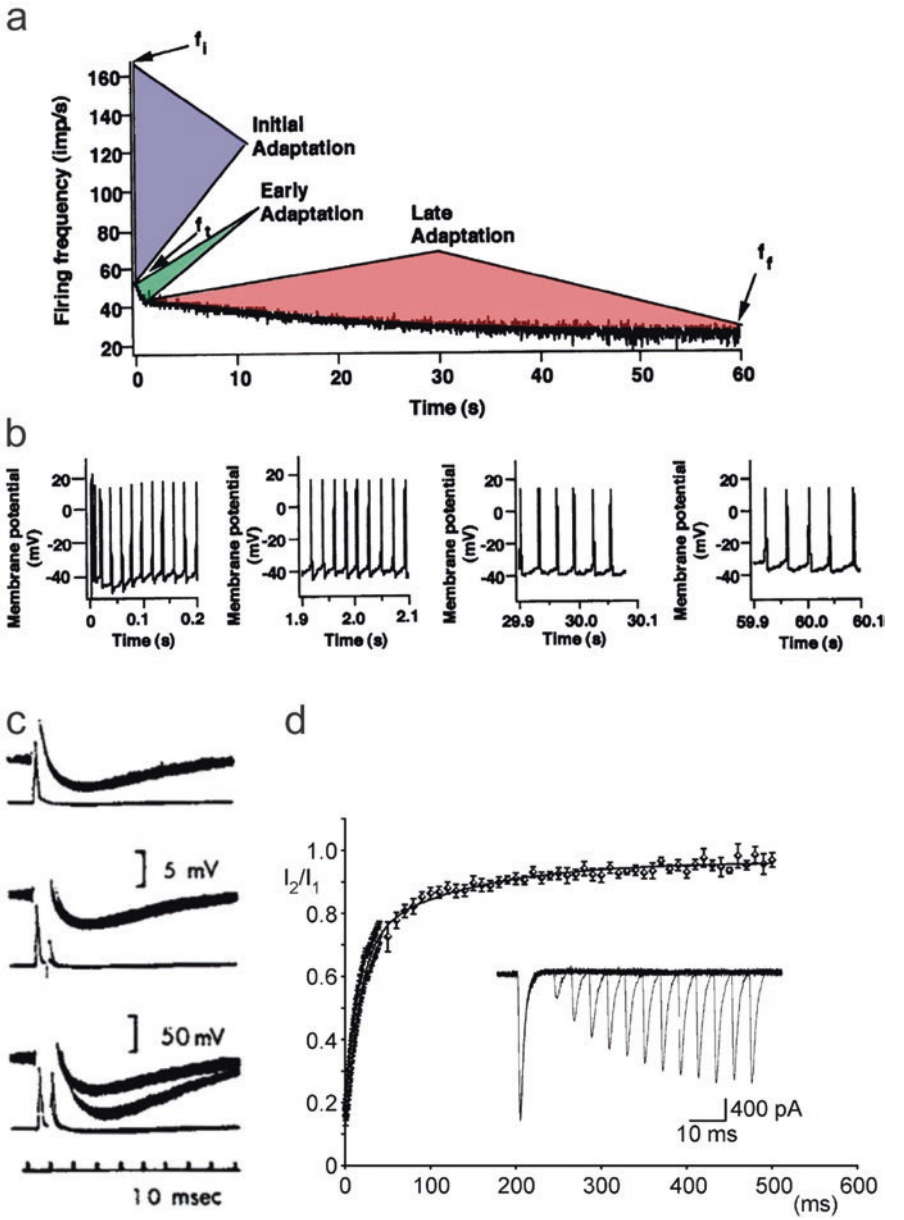

Fig. 5 Spike frequency adaptation and mAHP summation. (**a**) Firing rate in an adult rat hypoglossal motoneuron over the course of a 60s injected current pulse showing the initial frequency (f_i, *blue*), subsequent exponential decline (f_t, *green*) and slow decline (f_f, red) to final frequency, representing immediate (or initial), early, and late SFA. (**b**) 200 ms expanded samples of spiking show initial (first trace), early (second trace) and late (third-fourth traces) SFA. (**c**) AHP summation in an adult cat motoneuron. *Top panel*: AHP after single antidromic spike. *Middle panel*: no change

1963a; Kernell 1965), whereas late SFA occurs over many seconds to minutes (Kernell and Monster 1982; Fig. 5a, b). In addition, a third, earlier phase over a few spikes has been referred to as "immediate" SFA (Brownstone 2006). This phase results from the initial high instantaneous frequencies of initial doublets (see ADP section above), with subsequent intervals governed by the AHP (Sawczuk et al. 1995). SFA is more prominent in type F than type S motoneurons (Kernell 1972; Spielmann et al. 1993; Button et al. 2006).

Initially, early SFA was thought to arise from mAHP summation: the mAHP conductance is longer-lasting than the interspike interval, and would thus summate with that of the mAHP of the subsequent spike, leading to greater afterhyperpolarisation and a longer interspike interval (Fig. 5c; Ito and Oshima 1962; Baldissera and Gustafsson, 1971, 1974b). This concept was supported by computational studies (Baldissera and Gustafsson 1971, 1974a, b; Baldissera et al. 1978; Kernell and Sjöholm 1973; Kernell 1968, 1972).

On the other hand, it became clear that the mAHP was not completely responsible for SFA. Blocking calcium influx did not completely abolish early SFA (infact, it enhanced late SFA; Powers et al. 1999). These studies led to the suggestion that there are a number of potential mechanisms underlying SFA, including slow inactivation of sodium conductances and recruitment of other outward currents, such as an M-current (Powers et al. 1999). Further support for other mechanisms was found when blocking the AHP (SK) conductance in embryonic stem cell derived motoneurons did not alter early SFA (Miles et al. 2004). On noting that action potential amplitude progressively decreased, and duration increased throughout the spike train – both effects consistent with sodium channel inactivation – the time course of inactivation of Na^+ channels was studied and a slow component found, correlating with SFA (Fig. 5d; Miles et al. 2005). Furthermore, when incorporated into a computational model, the experimentally-determined slow inactivation parameters were sufficient to produce SFA (Miles et al. 2005). Thus, mechanisms underlying early SFA are likely multifactorial, with a slow time constant of sodium channel inactivation playing a significant role.

Late SFA, spanning seconds to minutes, is seen whether motoneurons are stimulated by continuous or repetitive stimulation (Stein and Parmiggiani 1979), and whether they are stimulated intracellularly (Kernell and Monster 1982) or extracellularly (Spielmann et al. 1993), suggesting that it is not an artefact produced by penetrating the membrane. The mechanisms contributing to late SFA are not clear, however slow inactivation of sodium channels is thought to contribute here as well (Brownstone 2006; Chen et al. 2006).

Fig 5 (continued) when a second spike fails to invade the soma. *Lower panel*: larger (summated) AHP when SD spike is elicited. In each panel, *upper trace* is amplification of *lower trace*. (**d**) Time course of recovery from sodium channel inactivation shown in a juvenile (P8–14) mouse motoneuron using a two pulse protocol. Note the (at least) double exponential of the recovery that parallels the phases of SFA. (**a** and **b**) Adapted from Sawczuk et al. (1995), Fig. 1. (**c**) from Ito and Oshima (1962), Fig. 1a–c. (**d**) from Miles et al. (2005), Fig. 5b

What are the functional consequences of SFA? On one hand, sustained high frequency firing is not necessary for optimal muscle contraction (Bigland-Ritchie et al. 1983a, b), and may even be detrimental to both the motoneuron and muscle fibre health (Vrbova 1983). Therefore, SFA could serve to protect motor units from excessive activation and subsequent damage. On the other hand, theories of motor unit rate coding suggest that SFA is a central mechanism contributing to motor fatigue (Kernell and Monster 1982; Gandevia 2001; Nordstrom et al. 2007). In this light, it is interesting that late SFA is reversed during fictive locomotion in cats and the reversal lasts even after the locomotor bout has finished, suggesting that it may be reversed by state dependent neuromodulatory inputs (Brownstone et al. 2011). If SFA does contribute to motor fatigue, a neuromodulatory system capable of supressing SFA would certainly be useful.

In summary, both early and late SFA represent fundamental characteristics of motoneuron repetitive firing and force control but their precise role in motor control remains unknown.

5 Modulation of Motoneuron Properties

Over the past several decades, it has become increasingly clear that motoneuron properties are not static, and that they can be modulated in a task-specific manner. While it is useful to study motoneuron properties in controlled, "quiescent," conditions to understand their basic properties and fundamental firing characteristics, these conditions do not reflect the state of motoneurons during behaviour when they are receiving both ionotropic and metabotropic (neuromodulatory) inputs.

We consider two main categories of modulation of motoneuron output: (a) output modulation, in which frequency of firing of the motoneuron in response to any given input is increased (i.e. agnostic to the specifics of the inputs), and (b) input modulation, which serves to alter the magnitude or duration of synaptic inputs received by the motoneuron. Thus, in broad terms, output modulation occurs at the soma, and in the case of motoneurons can be mediated by C-bouton synapses, and input modulation occurs at the dendrites and is often observed as persistent inward currents (PICs). Below we describe two best studied systems that contribute to output and input modulation of motoneuron activity.

Somatic Output Amplification: C-Bouton Synapses

C-boutons were first characterised anatomically as large synapses in apposition to α-motoneuron somata. They were named C-type boutons, or C-boutons, for the specialised endoplasmic reticulum, called sub surface cisternae (SSC), seen in proximity to the postsynaptic plasma membrane (Conradi 1969). C-boutons were later found to contain acetylcholine (Nagy et al. 1993). C-boutons were found to arise

from medial partition neurons, just lateral to the central canal (Miles et al. 2007), and identified as $V0_C$ interneurons that express the transcription factor Paired-like homeodomain 2 (Pitx2; Zagoraiou et al. 2009). Here, we consider C-bouton circuits to be output modulators as they alter the biophysical properties of motoneurons to increase excitability and thus frequency of firing.

$V0_C$ interneurons are active during fictive locomotion in neonatal spinal cord preparations (Nascimento et al. 2020; Zagoraiou et al. 2009) and appear to modulate fictive locomotor motoneuron bursting. However, in adult behaving mice, knock down of C-bouton transmission has no observed effect on over-ground locomotion (Zagoraiou et al. 2009). To date, the only behavioural deficit observed following C-bouton knock out is reduced EMG amplification between walking and swimming (Landoni et al. 2019; Zagoraiou et al. 2009), suggesting that C-boutons amplify motor output in a task-dependent manner. In other words, it is likely that C-boutons are important for high force output tasks, of which swimming is one example.

Acetylcholine released by $V0_C$ interneurons at C-bouton terminals binds to type 2 muscarinic acetylcholine receptors (M2Rs), which form dense aggregations spanning the apposing postsynaptic membrane (Hellström et al. 2003; Deardorff et al. 2013, 2014). Activation of M2Rs leads to an increase in motoneuron excitability (increased slope of f-I relationship, Miles et al. 2007), thought to be mediated via a number of factors at the complex postsynaptic domain. Studies from many labs have contributed to our understanding of the diversity of proteins associated with the post-synaptic site of C-bouton synapses (Fig. 6). These include: M2Rs (Hellström et al. 2003), SK2, SK3 (Deardorff et al. 2013) and $K_V2.1$ potassium channels (Muennich and Fyffe 2004), Sigma1 receptors (Mavlyutov et al. 2010), neuregulin-1 (Gallart-Palau et al. 2014), and TMEM16F (Soulard et al. 2020). It has been challenging to determine the role of each of these proteins in C-bouton physiology.

C-boutons are found on all limb innervating α- but not γ-motoneurons (Lagerbäck et al. 1986). A series of papers using electron microscopy to study the synaptology of fast and slow motoneurons (identified by intracellular recording of properties) in cats showed a relatively lower density of C-boutons on slow compared to fast motoneurons (Kellerth et al. 1979, 1983; Conradi et al. 1979). Furthermore, on fast motoneurons C-boutons organise into clusters around the dendritic roots and can be found on the axon hillock, whereas on slow motoneurons they tend to be restricted to the soma. The functional relevance of this organisational discrepancy is not clear.

SK Channels

Motoneurons express at least 2 types of SK channels that are responsible for the mAHP (see above). SK2 and SK3 channels are clustered post-synaptically to C-boutons but in different proportions in fast and slow motoneurons: all motoneurons express SK2 but smaller, slow type motoneurons express a higher level of SK3 (Deardorff et al. 2013). Based on the correlation between AHP amplitude and SK3 expression, this finding may explain the larger amplitude, longer duration mAHP in slow motoneurons (Zhang and Krnjević 1987; Hounsgaard and Mintz 1988).

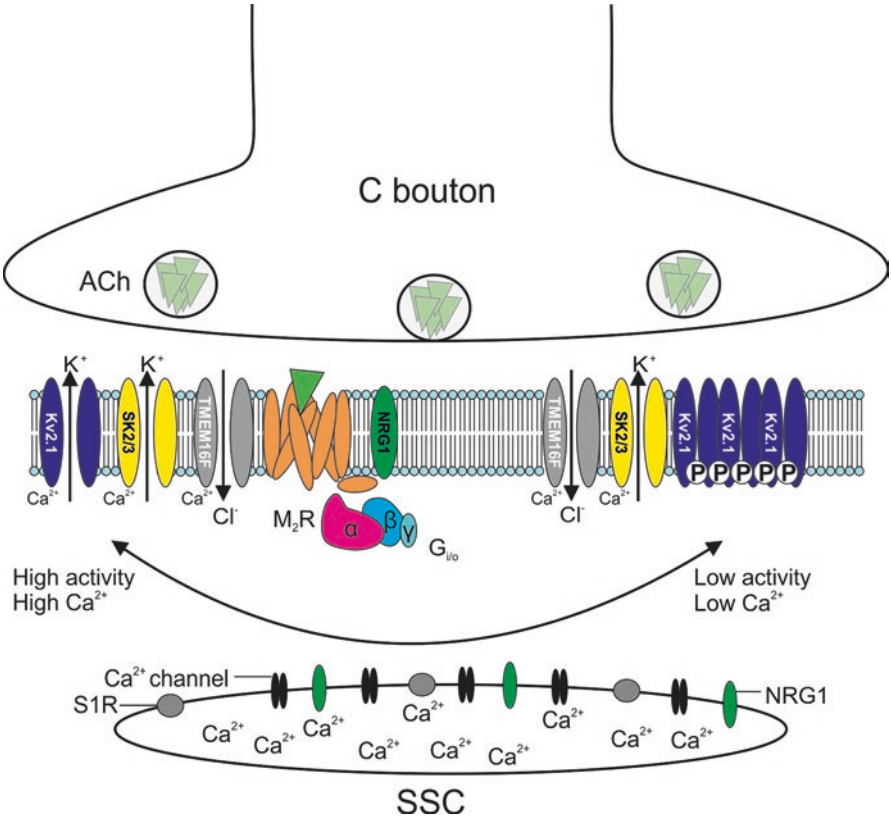

Fig. 6 C bouton organisation and hypothesised function. Presynaptic C-boutons release ACh which binds to M2 G-protein coupled receptors located in the motoneuron plasma membrane. Clustered together with M2 receptors are NRG1 proteins, SK2/3 and $K_V2.1$ potassium channels, and the chloride channel TMEM16F. Note that all channels post-synaptic to C boutons are calcium-dependent. $K_V2.1$ cycles between 2 states. During low activity, where intracellular Ca^{2+} is low, $K_V2.1$ channels are phosphorylated *(P)* and coalesce into large clusters, which are in a low or non-conducting state. With increasing activity leading to increases in intracellular Ca^{2+}, $K_V2.1$ is dephosphorylated and declustered, lowering its activation threshold and increasing K^+ conductance. SK2/3 and TMEM16F are activated by Ca^{2+} during high activity states. Just below the cell surface are the sub-surface cisterns (SSC), which are Ca^{2+} stores. Sigma-1 receptors and NRG1 proteins are primarily in the SSC membrane. M2 G-protein coupled receptor configurations is adapted Santiago and Abrol (2019), Fig. 1

Activation of M2Rs using pharmacological agonists in neonatal mouse spinal cord preparations reduces the mAHP, suggesting that the increase in *f*-I slope results from C-bouton-mediated reduction of SK conductance (Miles et al. 2007), either directly or indirectly (for example by reducing local calcium availability). It is not yet clear whether the source of local calcium is transmembrane, for example via Ca_V2-type Ca^{2+} currents (Li and Bennett 2007; Viana et al. 1993), or from an intracellular store like the adjacent SSC. In other neurons, ryanodine receptors have been found on SSC membranes and contribute to calcium induced calcium release

(Mandikian et al. 2014; Berridge 1998), but there is no evidence for their existence in motoneuronal SSC.

$K_V2.1$ Channels

K_V2 channels are delayed rectifier potassium channels that are widely expressed throughout the nervous system, contributing to the regulation of neuronal excitability (Misonou et al. 2005b; Du et al. 2000; Kihira et al. 2010). This family of voltage-gated potassium channels has 2 main isoforms, $K_V2.1$ and $K_V2.2$, that share many electrical properties. Likely due to a cloning artefact (see Kihira et al. 2010), $K_V2.2$ was initially thought to be restricted to distal dendritic compartments (Hwang et al. 1993), leaving $K_V2.1$ as the more studied isoform (Johnson et al. 2019).

In motoneurons, large clusters of $K_V2.1$ channels were discovered years ago (Muennich and Fyffe 2004), and are considered to be the main Kv2 isoform in these neurons (Deardorff et al. 2021; Romer et al. 2019). However, there is evidence that Kv2.2 is also expressed (Fletcher et al. 2017; Burger and Ribera 1996), although the exact membrane localisation and function has not been studied. Therefore, for the purposes of this chapter, we will focus on the Kv2.1 isoform.

Motoneuron $K_V2.1$ channels form large clusters at C-boutons, but their role in C-bouton physiology remains unclear (Muennich and Fyffe 2004). In the brain, due to the conductance's relatively slow activation/inactivation kinetics, $K_V2.1$ contributes significantly to the repolarisation of slow spiking neurons with broad action potentials (Liu and Bean 2014), but only minimally in faster spiking neurons (Guan et al. 2013; Du et al. 2000). On the other hand, $K_V2.1$ contributes to repetitive firing in all neuronal types studied, including motoneurons. All studies assessing $K_V2.1$ function in motoneurons so far use juvenile or neonatal in vitro preparations, before channels are fully clustered (Wilson et al. 2004), and none distinguishes between motoneuron type (e.g. fast vs. slow). A common finding is that inhibiting $K_V2.1$ channels with either Guangxitoxin 1-E (Fletcher et al. 2017; Nascimento et al. 2020) or stromatoxin (Romer et al. 2019) has no effect on the passive membrane properties of motoneurons. C-bouton-mediated increases in excitability are thought to be dependent on $K_V2.1$ channels (Nascimento et al. 2020), which may help to prevent gradual depolarisation of the interspike membrane voltage with repetitive firing, thereby reducing the depolarising block of sodium channels (Romer et al. 2019).

An interesting feature of $K_V2.1$ channels is that their state of clustering is dependent upon phosphorylation, which is regulated by Ca^{2+}/calcineurin dependent signalling mechanisms (Misonou et al. 2005a). In their clustered state, $K_V2.1$ channels either have higher activation thresholds (Murakoshi et al. 1997) and/or are non-conducting (Fox et al. 2013) – both effects decreasing potassium flux. An increase in neuronal activity and therefore calcium results in dephosphorylation of $K_V2.1$ channels, which increases their conductance by reducing activation threshold. One theory for $K_V2.1$ function in motoneurons is that C-boutons may act to inhibit local calcium activity, thus maintaining $K_V2.1$ clustering and maintaining basal rates of

potassium conductance (Romer et al. 2019). This would be sufficient to support high frequency firing by preventing depolarising block (Liu and Bean 2014; Nascimento et al. 2020; Romer et al. 2019). But in states of high frequency firing, increased intracellular calcium would de-cluster $K_V2.1$ channels, thereby reducing their activation threshold and thus homeostatically reduce firing frequency (Romer et al. 2019). However, we do not yet fully appreciate how $K_V2.1$ clustering at C-bouton synapses contributes to the modulatory role of these synapses.

Other Proteins Located at C-Bouton Synapses

There is even less understanding of the function of other proteins at this site. Transmembrane protein 16F (TMEM16F) was found to be responsible for a Ca^{2+} activated Cl^- current in cultured motoneurons, contributing to lowering recruitment thresholds of fast motoneurons in neonatal slice preparations. TMEM16F knockout mice had reduced maximum speed and endurance capacity during a treadmill running task, suggesting that they may be involved in C-bouton amplification of motor output.

Neuregulin 1 (NRG1) is also located post-synaptically at the SSC (Casanovas et al. 2017; Gallart-Palau et al. 2014; Issa et al. 2010). The function of NRG1 is poorly understood, but it may play a role in synaptic retrograde communication (Mòdol-Caballero et al. 2018) or in maintaining protein clustering at the synapse. Also located at the SSC are sigma-1 receptors (Mavlyutov et al. 2010, 2012) and their ligand Indole-*N*-methyl transferase (INMT), but there is little knowledge on the roles these proteins may play in C-bouton function.

In contrast to the lower density of SK3 on fast motoneurons (Deardorff et al. 2013), these neurons express the $K_V2.1$ β-subunit KCNG4 whereas slow motoneurons do not (Müller et al. 2014). The density of NRG1 clusters is higher in tibialis anterior motoneurons (fast) compared to soleus (slow), but the cluster size was larger in soleus (Casanovas et al. 2017). While the implications of these differences are not known, they emphasise the importance of studying known motoneuron types in order to provide further understanding of C-bouton function.

C-Boutons and Intracellular Calcium Signalling

C-boutons form complex synapses, with more localised proteins being discovered before the function of those previously known are understood. However, it is clear that Ca^{2+} is a key player in C-bouton function. To date, four Ca^{2+}-dependent ion channels (SK2, SK3, $K_V2.1$, and TMEM16F) have been identified, and SSC Ca^{2+} stores are located in close proximity. Future work aimed at characterising local Ca^{2+} fluxes during M2 receptor activation will undoubtedly provide insight into the intracellular signalling cascades underlying C-bouton mediated amplification of motor output.

Dendritic Input Amplification: Persistent Inward Currents

In 1975, Hultborn and colleagues demonstrated that, in response to brief trains of low threshold sensory afferent stimulation, cat motoneurons can produce "long latency prolonged activity", as shown in EMG and tension recordings (Hultborn et al. 1975). They proposed that this persistent activity could be due to a spinal interneuron circuit creating a reverberating excitatory loop. Schwindt and Crill (1977), using voltage clamp recordings in cat motoneurons, showed that these neurons had non-inactivating "N-shaped" current-voltage relationships, and that this property reflects a persistent net inward current (PIC, Fig. 7a–c). The group later suggested that PICs were generated "on or near the soma", and were mediated by calcium conductances (Schwindt and Crill 1980b, c, 1981). Following the Copenhagen group's demonstration of motoneuron plateau potentials and bistability produced by PICs (see section "Dendritic input amplification: persistent inward currents"; Hounsgaard et al. 1988a; Crone et al. 1988), and the implications of this activity for motor control, work spread to many labs and PICs have since been well-studied.

Persistent inward currents were initially thought to be produced solely by dihydropyridine-sensitive, non-inactivating calcium currents mediated by Ca_V1 (likely $Ca_V1.3$) channels (Perrier and Hounsgaard 2003; Hounsgaard and Kiehn 1985, 1993; Carlin et al. 2000). It was later demonstrated that persistent sodium currents (INaP; likely Nav1.1 and 1.6; Schwindt and Crill 1980a; Li and Bennett 2003) contribute to repetitive firing as well (Miles et al. 2005). That is, PICs are mediated by a combination of persistent sodium and calcium currents, and are modulated by metabotropic inputs (Li and Bennett 2003; Lee and Heckman 1999; Hounsgaard and Kiehn 1985; See Binder et al. 2020 for review).

There is now little doubt that PICs are generated primarily in motoneuron dendrites (Fig. 7c; Carlin et al. 2000, although it is possible that cooperative clustering of CaV1 channels on the soma contributes, Moreno et al. 2016). Having active conductances in the dendrites near the sites of synaptic inputs to motoneurons means that dendrites are not passive cables and, furthermore, provides a widespread substrate such that the responses to synaptic inputs can be modulated.

Modulation of PICs: Neurotransmitter Systems

It was initially curious that PICs or their effects had not been noted in the first decades of investigations of motoneuron properties. The likely reason for this "blind spot" was that motoneurons were usually investigated in anaesthetised preparations, and PICs are state-dependent, relying on modulatory inputs that are depressed by anaesthesia (Hounsgaard et al. 1986; Button et al. 2006). PICs are activated by monoaminergic, metabotropic neuromodulators, with the level of activation setting the degree of modulatory drive. The main source of these modulatory inputs are brain stem nuclei: raphe nuclei for serotonin (5HT; Conway et al. 1988; Hounsgaard

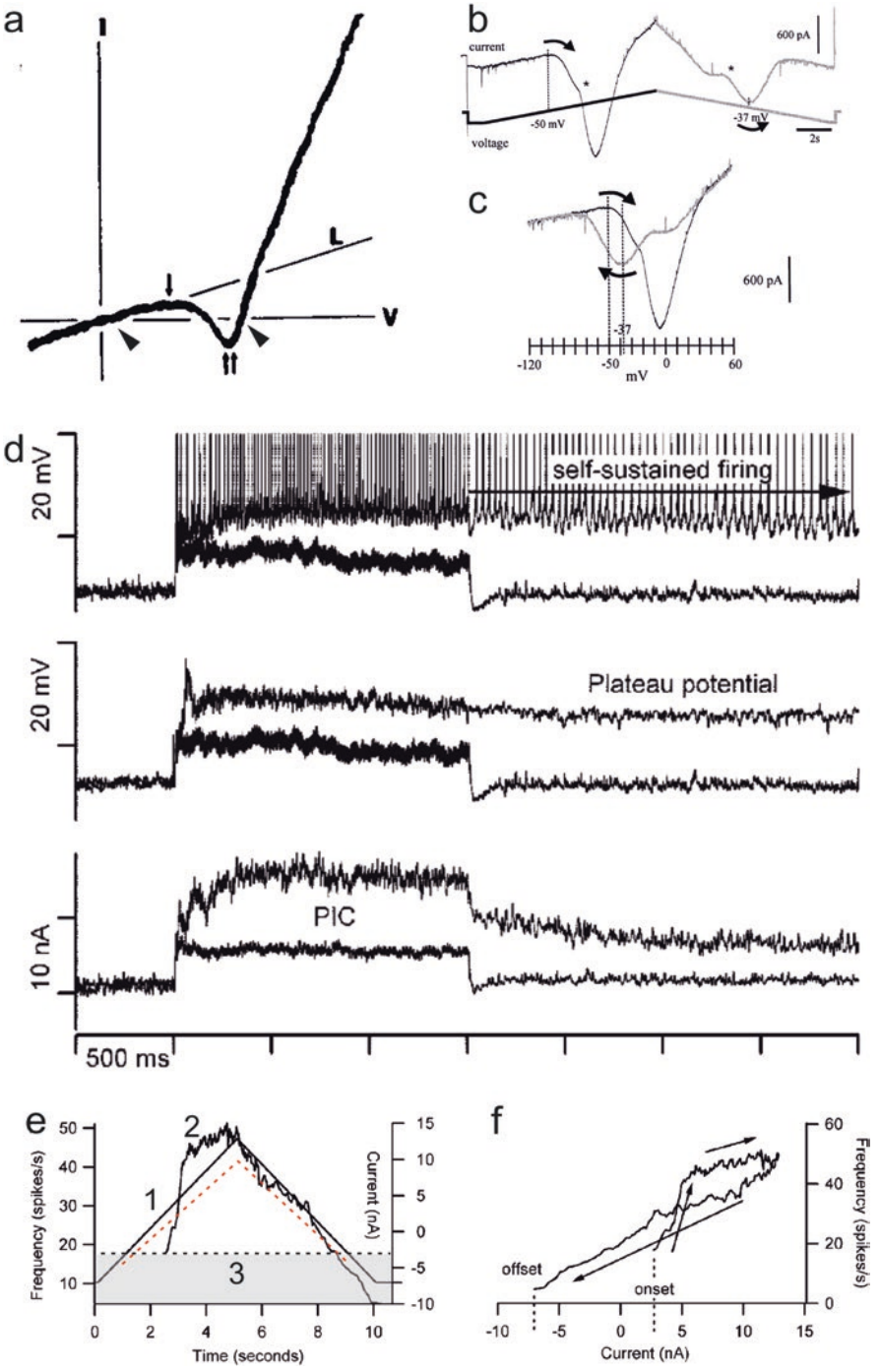
a
I
L
V
b
current
600 pA
-50 mV
-37 mV
voltage
2s
c
600 pA
-37
-120
-50
0
60
mV
d
20 mV
self-sustained firing
20 mV
Plateau potential
10 nA
PIC
500 ms
e
Frequency (spikes/s)
Current (nA)
1
2
3
Time (seconds)
f
offset
onset
Current (nA)
Frequency (spikes/s)

et al. 1988a; Alvarez et al. 1998), and the locus coeruleus for noradrenalin (NA; Björklund and Skagerberg 1982; Giroux et al. 1999; Conway et al. 1988). This is in contrast to output modulation by C-boutons, which is regulated by the evolutionarily older spinal cord. Not only are these systems depressed during anaesthesia, but they are modulated during changes in organismal state, increasing during wake as compared to sleep (Aston-Jones et al. 2000; Jacobs et al. 2002), and behavioural state, increasing during locomotion (Veasey et al. 1995). That is, these brain stem nuclei regulate PICs and thus dendritic integration in a state-dependent manner.

PICs, Repetitive Firing, and Synaptic Amplification

A key finding that led to our understanding of PICs arose from voltage clamp experiments in cats, in which N-shaped current-voltage (I–V) relations were found. The region of negative slope conductance in an N-shaped I–V relation is by definition unstable. But where the "N" crosses the abscissa with a positive slope (which can be at two different voltages depending on its position), the membrane potential will be stable – any small deviations will be counteracted by currents that bring the voltage back to this level (Schwindt and Crill 1980c). Furthermore, depolarisations from the more hyperpolarised "resting" membrane potential need only reach the "hump" of the N, or the unstable region, for the voltage to jump to the more depolarised stable

Fig. 7 (continued) N-shaped I–V relationship, PICs, and repetitive firing in motoneurons. (**a**) N-shaped I–V curve in an adult cat motoneuron revealed during slow depolarising ramp in voltage clamp. Slope of *line L* indicates passive leak conductance. *Single arrow* is first point of 0 slope conductance, and *double arrow* indicates maximum peak inward current. *Arrowheads* indicate abscissa crossings with positive slopes, which are stable voltages. (**b**) Current response to triangular voltage ramp in a juvenile (P8–15) mouse motoneuron in slice similarly reveals differences in 'N-shape' during ascending and descending ramps due to channel kinetics. * show inflection points, likely resulting from dendritic location of Ca_V1 channels. (**c**) These differences can be quantitatively appreciated when reflecting the response to the downward ramp (grey) on the upward ramp (black) to plot the I–V curve. The *dashed lines* indicate the onset of the region of negative slope conductance on the up-ramp, and the peak inward current on the down-ramp. (**d**) Voltage-dependent persistent inward currents generate plateau potentials and sustained firing in an adult cat motoneuron, with synaptic input activated by tendon vibration. The *top two panels* show voltage traces and the *lower panel* current traces. In each panel, the *lower trace* is when the cell held at hyperpolarised levels at which PICs are not activated, whereas the *top traces* are depolarised to voltages where PICs can be generated. The *top panel*, *top trace* illustrates self-sustained firing of a motoneuron activated by synaptic input. The *middle panel* shows the underlying plateau potential (*top trace*) in a motoneuron injected with QX-314 to block action potentials. In the *lower panel*, a PIC is initiated when the voltage is clamped at more depolarised levels. Note that the traces have been shifted along the y-axes, aligning the pre-pulse current/voltages to facilitate comparison. (**e**) Motoneuron model showing instantaneous firing frequency in response to a triangular current ramp in the absence (*red dashed line*) and presence (*solid, non-linear line*) of neuromodulation. *1–3* indicate major PIC phases. (**f**) *f*-I plot showing firing frequency hysteresis induced by PICs in an adult cat motoneuron. *Arrows* indicate direction of the change in current injection. (**a**) modified from Schwindt and Crill (1977), Fig. 1c. (**b** and **c**) from Carlin et al. (2000), Fig. 1b and c. (**d**) from Heckman et al. (2005), Fig. 2. (**e** and **f**) from Heckman et al. (2005), Fig. 4c–d

crossing. Thus, bistability is produced. But bistability is a special case – the inward and outward currents must be such that the N crosses the abscissa with a positive slope twice. In many motoneurons, this is unlikely to be the case and bistability is not seen (Heckman et al. 2003). Nonetheless, the voltage-gated channels responsible for PICs will amplify EPSPs, and, given that they are either slowly- or non-inactivating, the EPSPs will be prolonged and can impact temporal summation (Fig. 7d); In other words, in modulating these channels, brain stem monoaminergic systems can significantly change the integrative properties of motoneuron dendrites.

Of note, the recruitment of PICs parallels the transition from primary to secondary range firing (Schwindt and Crill 1982). In cats, the f-I slope of secondary range firing is higher than primary range, but some motoneurons do not have a secondary range. It is thought that counteracting factors such as increases in both spike threshold and outward potassium currents reduce the effects of the inward currents in those motoneurons (Schwindt and Crill 1982). Perhaps these forces are greater in mouse motoneurons, eliminating any PIC-mediated increase in f-I slope for secondary range firing.

These conductances also mean that less synaptic drive – in both amplitude and time – would be sufficient to ensure repetitive firing of motoneurons and hence muscle contraction. PICs can be strong enough to maintain firing in the absence of synaptic drive, until sufficient inhibition is received (Hounsgaard et al. 1988a; Lee and Heckman 2000; Hultborn et al. 2003).

The effects of PICs on motoneuron firing are clearly demonstrated during triangular current ramps (Fig. 7e, f). In the absence of PICs, motoneuron firing increases and decreases linearly with current input (Fig. 7e, red dashed line). However, when PICs are activated, firing accelerates rapidly, producing a steep *f*-I curve (*1.* Fig. 7e, non-linear line), followed by a reduction in the slope as maximum firing is approached (*2.* Fig. 7e), and finally a linear reduction in firing. These firing rate changes can be seen as an onset-offset hysteresis (*3.* Fig. 7e, f) of the *f*-I relationship (Hounsgaard et al. 1988a). Furthermore, the de-recruitment current threshold for firing is often lower than the recruitment threshold (*3.* Fig. 7e, shaded area shows difference), presumably due to slow/non inactivating PICs (Note that AHP prolongation may contribute to this effect as well; Wienecke et al. 2009). These voltage-dependent effects can also be seen during ramp current injections during locomotor activity, indicating that PICs or other voltage-dependent conductances are activated during synaptic excitation as well (Brownstone et al. 1994).

Termination of PICs

While persistent sodium currents are subject to slow inactivation (Lee and Heckman 1999), persistent calcium currents require strong inhibitory input or hyperpolarising/outward current to terminate them – to move to the left beyond the unstable region of negative slope conductance (Moritz et al. 2007; Perrier and Hounsgaard 2003; Hultborn et al. 1975). Furthermore, PICs are dependent on the balance between inward and outward K^+ currents (Schwindt and Crill 1980a, c, 1981), so any increase in K^+ current, such as a slowly activating K^+ current, can lead to their termination.

This can be mediated by SK channels through AHP summation (Li and Bennett 2007), or other potassium currents that are slowly-activating and non-inactivating, such as those mediated by KCNQ channels (M-currents; Alaburda et al. 2002). Renshaw cell inhibition is also well placed to terminate PICs (Bui et al. 2008).

PICs and Motor Pools

PIC channels are not homogeneously expressed across a motor pool and therefore contribute differently to sustained firing in different motoneuron types (Grande et al. 2007). Bistable behaviour (self-sustained firing, Fig. 7d) is more prevalent in low threshold slow motoneurons, in keeping with their fatigue resistance and involvement in sustained contractions such as those required for postural control (Eken and Kiehn 1989). Self-sustained firing is seldom seen in the largest, fast motoneurons, but this does not mean that they do not express PICs. In fact, PICs increase the gain of the f-I slope and reduce the decruitment threshold in these neurons as well. Hence, in fast, high threshold motoneurons, PICs primarily serve to amplify synaptic inputs, whereas in slow motoneurons they can also maintain repetitive firing.

6 Other Voltage- and Time- Varying Currents

Other non-linear properties of motoneurons can contribute to motoneuron repetitive firing. For example, during repeated phasic inputs, similar to those that occur during locomotion, a cumulative effect can lead to increasing firing frequency in response to the same input. This history-dependent increase in frequency is known as 'windup,' and although initially thought to be related to L-type Ca^{2+} channel activity, is seen even in neonatal motoneurons in which L-type Ca^{2+} channel expression is low, suggesting that other channels are involved (Pambo-Pambo et al. 2009). Indeed, motoneuron windup was found to be dependent on the nifedipine-sensitive K^+ channel, $K_V1.2$ (Bos et al. 2018). $K_V1.2$ is a slowly inactivating channel concentrated in the axon initial segment. Although present in most motoneurons, its slow ramping membrane depolarisation in response to rectangular current injection is preferentially seen in fast, high threshold motoneurons (Leroy et al. 2014). Thus, in response to long depolarising, near threshold, current injection (lasting seconds), fast motoneurons exhibit delayed firing (Fig. 8a) compared to slow motoneurons, which fire immediately (Fig. 8a1). In considering synaptic integration, fast motoneurons would thus be oblivious to low amplitude, near threshold inputs unless they were prolonged. $K_V1.2$ channels could therefore contribute to the observed size principle of recruitment (see Sect. 2). Furthermore, this finding has provided a surrogate marker to identify motoneuron type: long, near threshold current injections can distinguish fast from slow motoneurons by their delay to repetitive firing (Leroy et al. 2014; Fig. 8a–c1).

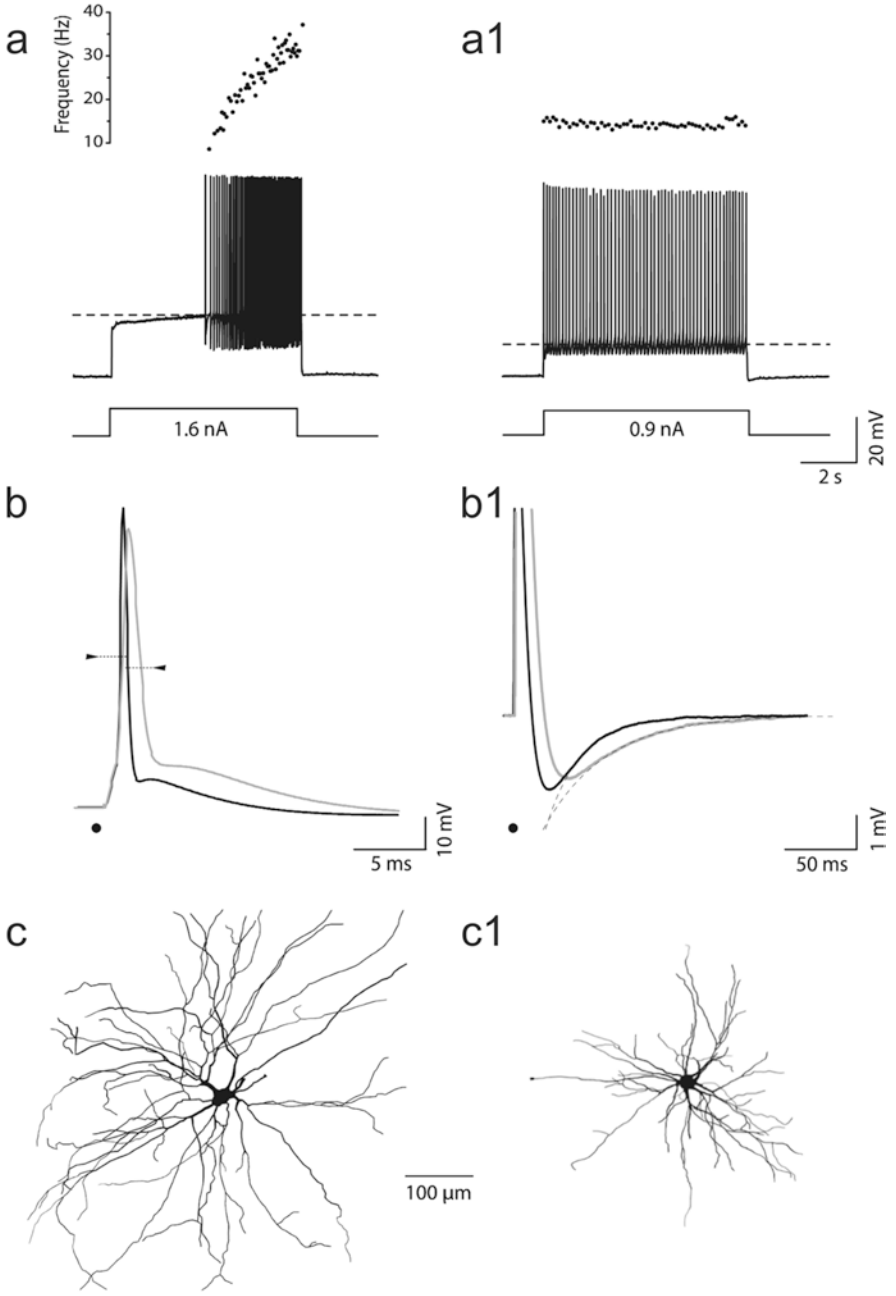

Fig. 8 Delayed and immediate firing motoneurons. Motoneurons may be categorized as fast or slow based on their threshold firing patterns during long duration rectangular current injections. (**a**) An example of a fast (6–10 day old) mouse motoneuron shows a ramping depolarisation in response to a stable near threshold current injection, resulting in delayed firing that increases in

The interaction of these slowly inactivating outward currents and SFA (see above) is interesting to consider, especially as both are more prominent in fast motoneurons (Spielmann et al. 1993; Button et al. 2006; Kernell 1972). Particularly in these motoneurons, it is therefore possible that for current injections in low suprathreshold ranges, the increases in firing rate resulting from inactivation of $K_V1.2$ could counterbalance decreases from SFA mechanisms (Brownstone et al. 2011). That is, at relatively low levels of current injections, SFA may not be seen (Fig. 8a; Leroy et al. 2014), whereas larger depolarisations would lead to clearer SFA (Sawczuk et al. 1995; Button et al. 2006).

7 Human Motor Unit Recordings

Our understanding of motoneuron physiology has been strengthened by the capacity to study motoneurons both in animals and in humans. Combining knowledge gained from experiments recording voluntary motor unit activity in humans with that gleaned from mechanistic studies in animal experiments has broadened our understanding of motoneuron physiology.

The first recordings of motor unit action potentials (MUAPs) from human muscle during voluntary contractions took place in the early 1900s (Wachholder 1928; see Duchateau & Enoka 2011 for comprehensive historical review). Adrian and Bronk (1929) used concentric needle electrodes to record single motor units, and provided an early description of rate coding, which describes the relationship between unit recruitment, spike frequency, and force output (Bigland and Lippold 1954). Development of fine wire electrodes for improving the signal to noise ratio of recordings (Stecko 1962) allowed principles of motoneuron physiology discovered in cat preparations, such as the size principle, to be studied during human voluntary contraction (Milner-Brown et al. 1973; Stein et al. 1972).

As humans can voluntarily produce different types of contractions with different magnitudes and rates of force generation, details about motor unit recruitment and rate coding could be readily studied (Büdingen and Freund 1976; Desmedt and Godaux 1977; Thomas et al. 1987). Subsequent investigations of motor unit firing patterns during different tasks enhanced our understanding of state-dependent motoneuron physiology (Collins et al. 2001). Thus, the fundamental knowledge from animal experiments could be interrogated in human motor units.

Fig 8 (continued) frequency over time. (**a1**) In slow motoneurons, action potential trains initiate at the onset of the input and spike frequencies do not accelerate. (**b**) Single action potentials in fast (*black*) motoneurons are shorter in duration (**b**) and have shorter mAHPs (**b1**) than slow (*grey*) motoneurons. These properties correspond to whether the motoneurons have delayed firing or not. (**c**) Analysis of motoneurons filled during recording demonstrates a larger dendritic tree in motoneurons with delayed (**c**) than those with immediate firing (**c1**), corresponding to the known characteristic that fast motoneurons are larger than slow motoneurons. (From Leroy et al. 2014)

Recently, much work has been directed toward recording multiple individual human motor units using intramuscular (Farina et al. 2008) and surface EMG electrode arrays (Holobar et al. 2009). These flexible, multi-channel EMG electrodes with tens of electrode contacts, combined with advances in signal processing algorithms led to the ability to record, decompose, and analyse most units in certain human muscles during isometric contractions (Farina et al. 2008; Muceli et al. 2018; Florestal et al. 2009; Marateb et al. 2011; Negro et al. 2016). This technique allowed for the comparison of activity in different motor units – for example early recruited (presumably S-type) vs late recruited (presumably F-type) units – which led to improved understanding of a motor pool. These studies revealed, for example, that while synaptic integration is non-linear in individual motoneurons, the population behaves linearly during these tasks (Farina and Negro 2015).

Development of these arrays and signal processing capacity to study human motor units has not only shed light on motor pool function in humans, but has allowed for the application of this technology in animals such as cat (Thompson et al. 2018) and song bird (Zia et al. 2018). This complementarity of human and animal studies is exemplary in demonstrating how the knowledge gained through such a combination is greater than the sum of each type of study independently.

Fatigue in Human Motoneurons

Muscle fatigue can be defined as the state occurring over time in which muscles have reduced contraction in response to a constant command, or in which an increase in command is needed to maintain a constant contraction. If that command is considered to originate at a pre-motoneuronal level, then a reduction in motoneuron responsiveness to that command could be considered a component of fatigue. Human studies of muscle fatigue have revealed that, during sustained voluntary contraction, there are two parallel components of fatigue: motor unit firing frequency decreases, and there is a concomitant decrease in the contractile properties of the innervated fibres. That is, the innervating motoneuron firing frequency reduces such that it does not fire at frequencies higher than that required for a fused tetanic contraction of its muscle fibre. Nonetheless, increasing the input to the motor pool by volitional control can increase motoneuron firing frequency during this fatigued state. The increase in command can recruit additional motor units in order to maintain the contraction, and likewise act on already recruited motoneurons to counterbalance reductions in firing frequency (Johnson et al. 2004). The degree to which descending modulatory activity changes and the roles that afferent input may play to enable motoneurons to increase their firing rate in these conditions are not known (Taylor et al. 2016).

But what are the cellular mechanisms behind this fatigue (Taylor et al. 2016; Enoka 2019)? Further studies on humans pointed to a central mechanism of fatigue, quite likely late spike frequency adaptation as seen in animal studies (Piotrkiewicz and Wilanowski 2012). As noted above, this late SFA can be reduced depending on behavioural state, such as when the animal is walking (Brownstone et al. 2011). As late SFA can be modulated, it may be that a strategy to "overcome" fatigue in the

short term would be to alter neuromodulatory state (consider a fight or flight reaction). Furthermore, this concept could lead to the suggestion that long term strategies to reduce fatiguing of muscles, such as exercise, may act through metamodulation, or changing the baseline modulatory state of motoneurons.

PICs in Human Motoneurons

One example where knowledge gleaned from animal studies has directly led to corresponding investigations of human motor unit physiology is the phenomenon of PICs (see section "Dendritic input amplification: persistent inward currents"). As with animal motoneurons recordings, in which PICs can be studied by ramp increases and decreases in injected current, human PICs can be approximated using a surrogate of injected current: ramp increases (and decreases) in voluntary force production. This paradigm was first used to study human motor units to demonstrate orderly recruitment, and high threshold units were found to have nonlinear firing (likely secondary range; De Luca et al. 1982). Interestingly, although long before PICs in animals were understood, a difference (decrease) between recruitment and derecruitment firing rates was shown (De Luca et al. 1982). In addition to onset-offset hysteresis, firing frequencies of motor units were found to accelerate (De Luca and Contessa 2012) and saturate (Fuglevand et al. 2015) on the ascending portion of the force ramp (De Luca et al. 1982; Mottram et al. 2009; Revill and Fuglevand 2017; Fig. 7e, 1–3). These phenomena all point towards PICs operating in human motoneurons.

To investigate PICs further, Gorassini et al. (2002) took advantage of the phenomenon that low threshold units can be used as a measure of synaptic input to the pool (Bennett et al. 1998; Lee et al. 2003), and developed quantitative methods for assessing PICs and f-I hysteresis in humans. For example, subjects were asked to maintain dorsiflexion at a small percentage of their maximal voluntary contraction (MVC) during recording of single units from the TA muscle, assuming that the same excitatory drive was being delivered to all motoneurons in the pool. Proprioceptive afferents, which project to all homonymous motoneurons, were then stimulated by tendon vibration to provide brief excitatory input to the pool. This led to recruitment and sustained firing in higher threshold TA motor units, presumably due to activation of PICs. On slowly reducing force, there was a reduction in firing rates of both low and higher threshold units. By using the firing frequency of the low threshold unit as a surrogate marker of drive to the pool, this "drive" at recruitment and derecruitment of the higher threshold unit could then be estimated. Indeed, firing rate hysteresis was found (lower drive at derecruitment than at recruitment), consistent with the proprioceptive input activating PICs. This technique was then validated in animal studies (Powers et al. 2008; Gorassini et al. 2002) and in computer simulations (Powers and Heckman 2015), and it is now widely used to assess excitability of human motoneurons in health (Herda et al. 2016) and disease states (Mottram et al. 2009, 2014). In addition, this technique has now been used to assess many motor units in a pool using high density EMG arrays (see beginning of Sect. 7), which have provided an additional, important dimension to our

understanding of human motoneuron physiology (Afsharipour et al. 2020). This knowledge will undoubtedly be enhanced by iterative approaches between the studies of animal and human motoneurons to gain mechanistic insights into human motor physiology.

8 Conclusion

Much progress has been made in our understanding of how motoneurons integrate synaptic inputs to produce trains of action potentials that stimulate muscles to contract with precise timing and force. This progress has been facilitated by experiments in both animals and humans, and the transfer of knowledge between the two. The fundamental basis of this knowledge derived from elegant work studying cat motoneuron physiology in vivo, and continues today largely in rodents in vitro and, to a lesser extent, in vivo. Mouse preparations have provided another dimension to our understanding through the capacity for genetic manipulation of motor circuits. Advances have also been made in our ability to record from motoneurons in behaving humans, allowing for the study of voluntary activation of motor pools.

But many questions remain. To understand behaviour, it is important to understand the fundamentals of movement. How are motoneuron properties tuned to the muscle fibre types they innervate? How do motoneurons integrate their many synaptic inputs to produce just the right amount of muscle contraction at a particular time and during a particular state? How do motoneuron pools work as an ensemble to ensure that joint angles change, or joints are stiffened, for the task at hand? How does the task-setting performed by higher centres change the modulatory state of motoneurons for the intended behaviour? These and other questions will be answered by ever expanding tools, interactions between those investigators of human and animal motoneuron function, and new, creative studies of this adaptable sensorimotor system.

References

Adrian ED, Bronk DW (1929) The discharge of impulses in motor nerve fibres: Part II. The frequency of discharge in reflex and voluntary contractions. J Physiol 67:9–151

Afsharipour B, Manzur N, Duchcherer J, Fenrich KF, Thompson CK, Negro F, Quinlan KA, Bennett DJ, Gorassini MA (2020) Estimation of self-sustained activity produced by persistent inward currents using firing rate profiles of multiple motor units in humans. J Neurophysiol 124:63–85

Alaburda A, Perrier JF, Hounsgaard J (2002) An M-like outward current regulates the excitability of spinal motoneurones in the adult turtle. J Physiol 540:875–881

Alvarez FJ, Pearson JC, Harrington D, Dewey D, Torbeck L, Fyffe RE (1998) Distribution of 5-hydroxytryptamine-immunoreactive boutons on α-motoneurons in the lumbar spinal cord of adult cats. J Comp Neurol 393:69–83

Araki T, Otani T (1955) Response of single motoneurons to direct stimulation in toad's spinal cord. J Neurophysiol 18:472–485

Aston-Jones G, Rajkowski J, Cohen J (2000) Locus coeruleus and regulation of behavioral flexibility and attention. Prog Brain Res. Elsevier

Baldissera F, Gustafsson B (1971) Regulation of repetitive firing in motoneurones by the afterhyperpolarization conductance. Brain Res 30:431–434

Baldissera BF, Gustafsson B (1974a) Afterhyperpolarization conductance time course in lumbar motoneurones of the cat. Acta Physiol Scand 91:512–527

Baldissera BF, Gustafsson B (1974b) Firing behaviour of a neurone model based on the afterhyperpolarization conductance time course. First interval firing. Acta Physiologica Scandinavica 91:528–544

Baldissera F, Gustafsson B, Parmiggiani F (1978) Saturating summation of the afterhyperpolarization conductance in spinal motoneurones: a mechanism for 'secondary range' repetitive firing. Brain Res 146:69–82

Baldissera F, Hultborn H, Illert M (1981) Integration in spinal neuronal systems. Compr Physiol

Barrett E, Barret J (1976) Separation of two voltage-sensitive potassium currents, and demonstration of a tetrodotoxin-resistant calcium current in frog motoneurones. J Physiol 255:737–774

Barrett J, Crill W (1980) Voltage clamp of cat motoneurone somata: properties of the fast inward current. J Physiol 304:231–249

Barron DH, Matthews BH (1938) The interpretation of potential changes in the spinal cord. J Physiol 92:276–321

Bayliss DA, Viana F, Bellingham MC, Berger AJ (1994) Characteristics and postnatal development of a hyperpolarization-activated inward current in rat hypoglossal motoneurons in vitro. J Neurophysiol 71:119–128

Bayliss DA, Umemiya M, Berger AJ (1995) Inhibition of N-and P-type calcium currents and the after-hyperpolarization in rat motoneurones by serotonin. J Physiol 485:635–647

Bennett DJ, Hultborn H, Fedirchuk B, Gorassini M (1998) Synaptic activation of plateaus in hindlimb motoneurons of decerebrate cats. J Neurophysiol 80:2023–2037

Berridge MJ (1998) Neuronal calcium signaling. Neuron 21:13–26

Bertrand S, Cazalets J-R (1998) Postinhibitory rebound during locomotor-like activity in neonatal rat motoneurons in vitro. J Neurophysiol 79:342–351

Bhumbra GS, Beato M (2018) Recurrent excitation between motoneurones propagates across segments and is purely glutamatergic. PLoS Biol 16:e2003586

Bigland B, Lippold O (1954) Motor unit activity in the voluntary contraction of human muscle. J Physiol 125:322–335

Bigland-Ritchie B, Johansson R, Lippold O, Woods J (1983a) Contractile speed and EMG changes during fatigue of sustained maximal voluntary contractions. J Neurophysiol 50:313–324

Bigland-Ritchie B, Johansson R, Lippold OCT, Smith S, Woods JJ (1983b) Changes in motoneurone firing rates during sustained maximal voluntary contractions. J Physiol 340:335–346

Binder MD, Powers RK, Heckman C (2020) Nonlinear input-output functions of motoneurons. Physiology 35:31–39

Björklund A, Skagerberg G (1982) Descending monoaminergic projections to the spinal cord. Brain Stem Control Spinal Mech:55–88

Bos R, Harris-Warrick RM, Brocard C, Demianenko LE, Manuel M, Zytnicki D, Korogod SM, Brocard F (2018) Kv1. 2 channels promote nonlinear spiking motoneurons for powering up locomotion. Cell Rep 22:3315–3327

Brock L, Coombs J, Eccles J (1951) Action potentials of motoneurones with intracellular electrode. Proc Univ Otago Med Sch:14–15

Brownstone RM (2006) Beginning at the end: repetitive firing properties in the final common pathway. Prog Neurobiol 78:156–172

Brownstone RM, Jordan L, Kriellaars D, Noga B, Shefchyk S (1992) On the regulation of repetitive firing in lumbar motoneurones during fictive locomotion in the cat. Exp Brain Res 90:441–455
Brownstone R, Gossard J-P, Hultborn H (1994) Voltage-dependent excitation of motoneurones from spinal locomotor centres in the cat. Exp Brain Res 102:34–44
Brownstone RM, Krawitz S, Jordan LM (2011) Reversal of the late phase of spike frequency adaptation in cat spinal motoneurons during fictive locomotion. J Neurophysiol 105:1045–1050
Büdingen HJ, Freund H-J (1976) The relationship between the rate of rise of isometric tension and motor unit recruitment in a human forearm muscle. Pflugers Arch 362:61–67
Bui TV, Grande G, Rose PK (2008) Relative location of inhibitory synapses and persistent inward currents determines the magnitude and mode of synaptic amplification in motoneurons. J Neurophysiol 99:583–594
Burger C, Ribera AB (1996) Xenopus spinal neurons express Kv2 potassium channel transcripts during embryonic development. J Neurosci 16:1412–1421
Burke RE (1967) Composite nature of the monosynaptic excitatory postsynaptic potential. J Neurophysiol 30:1114–1137
Burke R, Glenn LL (1996) Horseradish peroxidase study of the spatial and electrotonic distribution of group Ia synapses on type-identified ankle extensor motoneurons in the cat. J Comp Neurol 372:465–485
Burke R, Rudomin P, Zajac F (1970) Catch property in single mammalian motor units. Science 168:122–124
Burke R, Levine D, Tsairis P, Zajac F III (1973) Physiological types and histochemical profiles in motor units of the cat gastrocnemius. J Physiol 234:723–748
Button DC, Gardiner K, Marqueste T, Gardiner PF (2006) Frequency–current relationships of rat hindlimb α-motoneurones. J Physiol 573:663–677
Canto-Bustos M, Loeza-Alcocer E, González-Ramírez R, Gandini MA, Delgado-Lezama R, Felix R (2014) Functional expression of T-type ca 2+ channels in spinal motoneurons of the adult turtle. PLoS One 9:e108187
Carlin K, Jones K, Jiang Z, Jordan L, Brownstone R (2000) Dendritic L-type calcium currents in mouse spinal motoneurons: implications for bistability. Eur J Neurosci 12:1635–1646
Casanovas A, Salvany S, Lahoz V, Tarabal O, Piedrafita L, Sabater R, Hernández S, Calderó J, Esquerda JE (2017) Neuregulin 1-ErbB module in C-bouton synapses on somatic motor neurons: molecular compartmentation and response to peripheral nerve injury. Sci Rep 7:1–17
Chandler SH, Hsaio C-F, Inoue T, Goldberg LJ (1994) Electrophysiological properties of Guinea pig trigeminal motoneurons recorded in vitro. J Neurophysiol 71:129–145
Chen Y, Frank HY, Surmeier DJ, Scheuer T, Catterall WA (2006) Neuromodulation of Na+ channel slow inactivation via cAMP-dependent protein kinase and protein kinase C. Neuron 49:409–420
Collins D, Burke D, Gandevia S (2001) Large involuntary forces consistent with plateau-like behavior of human motoneurons. J Neurosci 21:4059–4065
Conradi S (1969) Ultrastructure and distribution of neuronal and glial elements on the surface of the proximal part of a motoneuron dendrite, as analyzed by serial sections. Acta Physiol Scand Suppl 332:49
Conradi S, Kellerth JO, Berthold CH, Hammarberg C (1979) Electron microscopic studies of serially sectioned cat spinal α-motoneurons. IV. Motoneurons innervating slow-twitch (type s) units of the soleus muscle. J Comp Neurol 184:769–782
Conway B, Hultborn H, Kiehn O, Mintz I (1988) Plateau potentials in alpha-motoneurones induced by intravenous injection of L-dopa and clonidine in the spinal cat. J Physiol 405:369–384
Coombs J, Curtis D, Eccles J (1957) The interpretation of spike potentials of motoneurones. J Physiol 139:198–231
Cooper S, Eccles J (1930) The isometric responses of mammalian muscles. J Physiol 69:377–385
Crone C, Hultborn H, Kiehn O, Mazieres L, Wigström H (1988) Maintained changes in motoneuronal excitability by short-lasting synaptic inputs in the decerebrate cat. J Physiol 405:321–343

De Luca CJ, Contessa P (2012) Hierarchical control of motor units in voluntary contractions. J Neurophysiol 107:178–195
De Luca C, Lefever R, Mccue M, Xenakis A (1982) Behaviour of human motor units in different muscles during linearly varying contractions. J Physiol 329:113–128
Deardorff AS, Romer SH, Deng Z, Bullinger KL, Nardelli P, Cope TC, Fyffe RE (2013) Expression of postsynaptic Ca2+-activated K+ (SK) channels at C-bouton synapses in mammalian lumbar α-motoneurons. J Physiol 591:875–897
Deardorff AS, Romer SH, Sonner PM, Fyffe RE (2014) Swimming against the tide: investigations of the C-bouton synapse. Front Neural Circ 8:106
Deardorff AS, Romer SH, Fyffe RE (2021) Location, location, location: the organization and roles of potassium channels in mammalian motoneurons. J Physiol 599:1391–1420
Desmedt JE, Godaux E (1977) Ballistic contractions in man: characteristic recruitment pattern of single motor units of the tibialis anterior muscle. J Physiol 264:673–693
Dodt H-U, Zieglgänsberger W (1990) Visualizing unstained neurons in living brain slices by infrared DIC-videomicroscopy. Brain Res 537:333–336
Du J, Haak LL, Phillips-Tansey E, Russell JT, Mcbain CJ (2000) Frequency-dependent regulation of rat hippocampal somato-dendritic excitability by the K+ channel subunit Kv2. 1. J Physiol 522:19–31
Duflocq A, Le Bras B, Bullier E, Couraud F, Davenne M (2008) Nav1. 1 is predominantly expressed in nodes of Ranvier and axon initial segments. Mol Cell Neurosci 39:180–192
Duflocq A, Chareyre F, Giovannini M, Couraud F, Davenne M (2011) Characterization of the axon initial segment (AIS) of motor neurons and identification of a para-AIS and a juxtapara-AIS, organized by protein 4.1 B. BMC Biol 9:1–19
Eccles J (1961) Membrane time constants of cat motoneurons and time courses of synaptic action. Exp Neurol 4:1–22
Eccles JC, Hoff H (1932) The rhythmic discharge of motoneurones. Proc R Soc Lond Ser B Contain Pap Biol Character 110:483–514
Eccles JC, Eccles RM, Lundberg A (1958) The action potentials of the alpha motoneurones supplying fast and slow muscles. J Physiol 142:275–291
Edwards FA, Konnerth A, Sakmann B, Takahashi T (1989) A thin slice preparation for patch clamp recordings from neurones of the mammalian central nervous system. Pflugers Arch 414:600–612
Eken T, Kiehn O (1989) Bistable firing properties of soleus motor units in unrestrained rats. Acta Physiol Scand 136:383–394
Enoka RM (2019) Physiological validation of the decomposition of surface EMG signals. J Electromyogr Kinesiol 46:70–83
Evinger C (1988) Extraocular motor nuclei: location, morphology and afferents. Rev Oculomot Res 2:81–117
Farina D, Negro F (2015) Common synaptic input to motor neurons, motor unit synchronization, and force control. Exerc Sport Sci Rev 43:23–33
Farina D, Yoshida K, Stieglitz T, Koch KP (2008) Multichannel thin-film electrode for intramuscular electromyographic recordings. J Appl Physiol 104:821–827
Fletcher EV, Simon CM, Pagiazitis JG, Chalif JI, Vukojicic A, Drobac E, Wang X, Mentis GZ (2017) Reduced sensory synaptic excitation impairs motor neuron function via Kv2. 1 in spinal muscular atrophy. Nat Neurosci
Florestal J, Mathieu P, Mcgill K (2009) Automatic decomposition of multichannel intramuscular EMG signals. J Electromyogr Kinesiol 19:1–9
Fox PD, Loftus RJ, Tamkun MM (2013) Regulation of Kv2. 1 K+ conductance by cell surface channel density. J Neurosci 33:1259–1270
Fuglevand AJ, Lester RA, Johns RK (2015) Distinguishing intrinsic from extrinsic factors underlying firing rate saturation in human motor units. J Neurophysiol 113:1310–1322

Fukuda S, Maeda H, Sakurai M (2020) Reevaluation of motoneuron morphology: diversity and regularity among motoneurons innervating different arm muscles along a proximal–distal axis. Sci Rep 10:1–10

Fuortes M, Frank K, Becker MC (1957) Steps in the production of motoneuron spikes. J Gen Physiol 40:735–752

Gallart-Palau X, Tarabal O, Casanovas A, Sábado J, Correa FJ, Hereu M, Piedrafita L, Calderó J, Esquerda JE (2014) Neuregulin-1 is concentrated in the postsynaptic subsurface cistern of C-bouton inputs to α-motoneurons and altered during motoneuron diseases. FASEB J 28:3618–3632

Gandevia SC (2001) Spinal and supraspinal factors in human muscle fatigue. Physiol Rev 81:1725–1789

Garland SJ, Griffin L (1999) Motor unit double discharges: statistical anomaly or functional entity? Can J Appl Physiol 24:113–130

Garrido JJ, Giraud P, Carlier E, Fernandes F, Moussif A, Fache M-P, Debanne D, Dargent B (2003) A targeting motif involved in sodium channel clustering at the axonal initial segment. Science 300:2091–2094

Gestreau C, Dutschmann M, Obled S, Bianchi AL (2005) Activation of XII motoneurons and premotor neurons during various oropharyngeal behaviors. Respir Physiol Neurobiol 147:159–176

Giroux N, Rossignol S, Reader TA (1999) Autoradiographic study of α1-and α2-noradrenergic and serotonin1A receptors in the spinal cord of normal and chronically transected cats. J Comp Neurol 406:402–414

Gorassini M, Yang JF, Siu M, Bennett DJ (2002) Intrinsic activation of human motoneurons: possible contribution to motor unit excitation. J Neurophysiol 87:1850–1858

Grande G, Bui TV, Rose PK (2007) Estimates of the location of L-type Ca2+ channels in motoneurons of different sizes: a computational study. J Neurophysiol 97:4023–4035

Granit R (1975) The functional role of the muscle spindles – facts and hypotheses. Brain J Neurol 98:531–556

Granit R, Kernell D, Shortess G (1963a) Quantitative aspects of repetitive firing of mammalian motoneurones, caused by injected currents. J Physiol 168:911–931

Granit R, Kernell D, Smith R (1963b) Delayed depolarization and the repetitive response to intracellular stimulation of mammalian motoneurones. J Physiol 168:890–910

Granit R, Kernell D, Lamarre Y (1966a) Algebraical summation in synaptic activation of motoneurones firing within the 'primary range' to injected currents. J Physiol 187:379–399

Granit R, Kernell D, Lamarre Y (1966b) Synaptic stimulation superimposed on motoneurones firing in the 'secondary range' to injected current. J Physiol 187:401–415

Guan D, Armstrong WE, Foehring RC (2013) Kv2 channels regulate firing rate in pyramidal neurons from rat sensorimotor cortex. J Physiol 591:4807–4825

Heckman C, Lee RH, Brownstone RM (2003) Hyperexcitable dendrites in motoneurons and their neuromodulatory control during motor behavior. Trends Neurosci 26:688–695

Heckman C, Gorassini MA, Bennett DJ (2005) Persistent inward currents in motoneuron dendrites: implications for motor output. Muscle Nerve 31:135–156

Hellström J, Oliveira AL, Meister B, Cullheim S (2003) Large cholinergic nerve terminals on subsets of motoneurons and their relation to muscarinic receptor type 2. J Comp Neurol 460:476–486

Henneman E (1957) Relation between size of neurons and their susceptibility to discharge. Science 126:1345–1347

Herda T, Miller J, Trevino M, Mosier E, Gallagher P, Fry A, Vardiman J (2016) The change in motor unit firing rates at de-recruitment relative to recruitment is correlated with type I myosin heavy chain isoform content of the vastus lateralis in vivo. Acta Physiol 216:454–463

Hochman S, Jordan LM, Schmidt BJ (1994) TTX-resistant NMDA receptor-mediated voltage oscillations in mammalian lumbar motoneurons. J Neurophysiol 72:2559–2562

Hodgkin AL, Huxley AF (1939) Action potentials recorded from inside a nerve fibre. Nature 144:710–711

Holobar A, Farina D, Gazzoni M, Merletti R, Zazula D (2009) Estimating motor unit discharge patterns from high-density surface electromyogram. Clin Neurophysiol 120:551–562
Hounsgaard J, Kiehn O (1985) Ca++ dependent bistability induced by serotonin in spinal motoneurons. Exp Brain Res 57:422–425
Hounsgaard J, Kiehn O (1993) Calcium spikes and calcium plateaux evoked by differential polarization in dendrites of turtle motoneurones in vitro. J Physiol 468:245–259
Hounsgaard J, Mintz I (1988) Calcium conductance and firing properties of spinal motoneurones in the turtle. J Physiol 398:591–603
Hounsgaard J, Hultborn H, Kiehn O (1986) Transmitter-controlled properties of α-motoneurones causing long-lasting motor discharge to brief excitatory inputs. Prog Brain Res. Elsevier
Hounsgaard J, Hultborn H, Jespersen B, Kiehn O (1988a) Bistability of alpha-motoneurones in the decerebrate cat and in the acute spinal cat after intravenous 5-hydroxytryptophan. J Physiol 405:345–367
Hounsgaard J, Kiehn O, Mintz I (1988b) Response properties of motoneurones in a slice preparation of the turtle spinal cord. J Physiol 398:575–589
Hultborn H, Wigström H, Wängberg B (1975) Prolonged activation of soleus motoneurones following a conditioning train in soleus Ia afferents – a case for a reverberating loop? Neurosci Lett 1:147–152
Hultborn H, Denton ME, Wienecke J, Nielsen JB (2003) Variable amplification of synaptic input to cat spinal motoneurones by dendritic persistent inward current. J Physiol 552:945–952
Hwang P, Cunningham A, Peng Y, Snyder S (1993) CDRK and DRK1 K+ channels have contrasting localizations in sensory systems. Neuroscience 55:613–620
Iansek R, Redman S (1973a) The amplitude, time course and charge of unitary excitatory postsynaptic potentials evoked in spinal motoneurone dendrites. J Physiol 234:665–688
Iansek R, Redman S (1973b) An analysis of the cable properties of spinal motoneurones using a brief intracellular current pulse. J Physiol 234:613–636
Iglesias C, Meunier C, Manuel M, Timofeeva Y, Delestrée N, Zytnicki D (2011) Mixed mode oscillations in mouse spinal motoneurons arise from a low excitability state. J Neurosci 31:5829–5840
Issa AN, Zhan WZ, Sieck GC, Mantilla CB (2010) Neuregulin-1 at synapses on phrenic motoneurons. J Comp Neurol 518:4213–4225
Ito M, Oshima T (1962) Temporal summation of after-hyperpolarization following a motoneurone spike. Nature 195:910–911
Jacques, Duchateau Roger M., Enoka (2011) Human motor unit recordings: Origins and insight into the integrated motor system. Brain Research 140942-61 10.1016/j.brainres.2011.06.011
Jacobs BL, Martín-Cora FJ, Fornal CA (2002) Activity of medullary serotonergic neurons in freely moving animals. Brain Res Rev 40:45–52
Jensen DB, Stecina K, Wienecke J, Hedegaard A, Sukiasyan N, Hultborn HR, Meehan CF (2018) The subprimary range of firing is present in both cat and mouse spinal motoneurons and its relationship to force development is similar for the two species. J Neurosci 38:9741–9753
Jensen DB, Kadlecova M, Allodi I, Meehan CF (2020) Spinal motoneurones are intrinsically more responsive in the adult G93A SOD1 mouse model of Amyotrophic Lateral Sclerosis. J Physiol 598:4385–4403
Johnson K, Edwards S, Van Tongeren C, Bawa P (2004) Properties of human motor units after prolonged activity at a constant firing rate. Exp Brain Res 154:479–487
Johnson B, Leek AN, Tamkun MM (2019) Kv2 channels create endoplasmic reticulum/plasma membrane junctions: a brief history of Kv2 channel subcellular localization. Channels 13:88–101
Kanning KC, Kaplan A, Henderson CE (2010) Motor neuron diversity in development and disease. Annu Rev Neurosci 33:409–440
Kellerth JO, Berthold CH, Conradi S (1979) Electron microscopic studies of serially sectioned cat spinal α-motoneurons. III. Motoneurons innervating fast-twitch (type FR) units of the gastrocnemius muscle. J Comp Neurol 184:755–767

Kellerth JO, Conradi S, Berthold CH (1983) Electron microscopic studies of serially sectioned cat spinal α-motoneurons: V. motoneurons innervating fast-twitch (type FF) units of the gastrocnemius muscle. J Comp Neurol 214:451–458

Kernell D (1964) The delayed depolarization in cat and rat motoneurones. Prog Brain Res. Elsevier

Kernell D (1965) Synaptic influence on the repetitive activity elicited in cat lumbosacral motoneurones by long-lasting injected currents. Acta Physiol Scand 63:409–410

Kernell D (1968) The repetitive impulse discharge of a simple neurone model compared to that of spinal motoneurones. Brain Res 11:685–687

Kernell D (1972) The early phase of adaptation in repetitive impulse discharges of cat spinal motoneurones. Brain Res 41:184–186

Kernell D (1983) Functional properties of spinal motoneurons and gradation of muscle force. Adv Neurol 39:213–226

Kernell D (1999) Repetitive impulse firing in motoneurons: facts and perspectives. Prog Brain Res 123:31–37

Kernell D (2006) The motoneurone and its muscle fibres

Kernell D, Monster A (1982) Time course and properties of late adaptation in spinal motoneurones of the cat. Exp Brain Res 46:191–196

Kernell D, Sjöholm H (1973) Repetitive impulse firing: comparisons between neurone models based on 'voltage clamp equations' and spinal motoneurones. Acta Physiol Scand 87:40–56

Kihira Y, Hermanstyne TO, Misonou H (2010) Formation of heteromeric Kv2 channels in mammalian brain neurons. J Biol Chem 285:15048–15055

Kleinfeld D, Moore JD, Wang F, Deschênes M (2014) The brainstem oscillator for whisking and the case for breathing as the master clock for orofacial motor actions. In: Cold Spring Harbor symposia on quantitative biology. Cold Spring Harbor Laboratory Press, pp 29–39

Kobayashi M, Inoue T, Matsuo R, Masuda Y, Hidaka O, Kang Y, Morimoto T (1997) Role of calcium conductances on spike afterpotentials in rat trigeminal motoneurons. J Neurophysiol 77:3273–3283

Kolmodin G, Skoglund C (1958) Slow membrane potential changes accompanying excitaltion and inhibition in spinal noto-and interneurons in the cat during natural activation. Acta Physiol Scand 44:11–54

Konishi S, Otsuka M (1974) Excitatory action of hypothalamic substance P on spinal motoneurones of newborn rats. Nature 252:734

Krawitz S, Fedirchuk B, Dai Y, Jordan L, Mccrea D (2001) State-dependent hyperpolarization of voltage threshold enhances motoneurone excitability during fictive locomotion in the cat. J Physiol 532:271–281

Krnjević K, Lamour Y, Macdonald J, Nistri A (1978) Motoneuronal after-potentials and extracellular divalent cations. Can J Physiol Pharmacol 56:516–520

Krutki P, Mrówczyński W, Bączyk M, Łochyński D, Celichowski J (2017) Adaptations of motoneuron properties after weight-lifting training in rats. J Appl Physiol 123:664–673

Lagerbäck P-Å, Cullheim S, Ulfhake B (1986) Electron microscopic observations on the synaptology of cat sciatic γ-motoneurons after intracellular staining with horseradish peroxidase. Neurosci Lett 70:23–27

Landoni LM, Myles JR, Wells TL, Mayer WP, Akay T (2019) Cholinergic modulation of motor neurons through the C-boutons are necessary for the locomotor compensation for severe motor neuron loss during amyotrophic lateral sclerosis disease progression. Behav Brain Res 369:111914

Larkman P, Kelly J (1992) Ionic mechanisms mediating 5-hydroxytryptamine-and noradrenaline-evoked depolarization of adult rat facial motoneurones. J Physiol 456:473–490

Le Bras B, Fréal A, Czarnecki A, Legendre P, Bullier E, Komada M, Brophy PJ, Davenne M, Couraud F (2014) In vivo assembly of the axon initial segment in motor neurons. Brain Struct Funct 219:1433–1450

Lee R, Heckman C (1999) Paradoxical effect of QX-314 on persistent inward currents and bistable behavior in spinal motoneurons in vivo. J Neurophysiol 82:2518–2527

Lee RH, Heckman CJ (2000) Adjustable amplification of synaptic input in the dendrites of spinal motoneurons in vivo. J Neurosci 20:6734–6740
Lee R, Kuo J, Jiang M, Heckman C (2003) Influence of active dendritic currents on input-output processing in spinal motoneurons in vivo. J Neurophysiol 89:27–39
Leroy F, D'incamps BL, Imhoff-Manuel RD, Zytnicki D (2014) Early intrinsic hyperexcitability does not contribute to motoneuron degeneration in amyotrophic lateral sclerosis. Elife 3:e04046
Li Y, Bennett DJ (2003) Persistent sodium and calcium currents cause plateau potentials in motoneurons of chronic spinal rats. J Neurophysiol 90:857–869
Li X, Bennett DJ (2007) Apamin-sensitive calcium-activated potassium currents (SK) are activated by persistent calcium currents in rat motoneurons. J Neurophysiol 97:3314–3330
Li W-C, Soffe SR, Roberts A (2004a) A direct comparison of whole cell patch and sharp electrodes by simultaneous recording from single spinal neurons in frog tadpoles. J Neurophysiol
Li Y, Gorassini MA, Bennett DJ (2004b) Role of persistent sodium and calcium currents in motoneuron firing and spasticity in chronic spinal rats. J Neurophysiol 91:767–783
Liddell EGT, Sherrington C (1924) Reflexes in response to stretch (myotatic reflexes). Proc R Soc Lond Ser B Contain Pap Biol Character 96:212–242
Liu PW, Bean BP (2014) Kv2 channel regulation of action potential repolarization and firing patterns in superior cervical ganglion neurons and hippocampal CA1 pyramidal neurons. J Neurosci 34:4991–5002
Lorincz A, Nusser Z (2008) Cell-type-dependent molecular composition of the axon initial segment. J Neurosci 28:14329–14340
Mandikian D, Bocksteins E, Parajuli LK, Bishop HI, Cerda O, Shigemoto R, Trimmer JS (2014) Cell type–specific spatial and functional coupling between mammalian brain Kv2. 1 K+ channels and ryanodine receptors. J Comp Neurol 522:3555–3574
Manuel M, Heckman C (2011) Adult mouse motor units develop almost all of their force in the subprimary range: a new all-or-none strategy for force recruitment? J Neurosci 31:15188–15194
Manuel M, Iglesias C, Donnet M, Leroy F, Heckman C, Zytnicki D (2009) Fast kinetics, high-frequency oscillations, and subprimary firing range in adult mouse spinal motoneurons. J Neurosci 29:11246–11256
Marateb HR, Muceli S, Mcgill KC, Merletti R, Farina D (2011) Robust decomposition of single-channel intramuscular EMG signals at low force levels. J Neural Eng 8:066015
Mavlyutov TA, Epstein ML, Andersen KA, Ziskind-Conhaim L, Ruoho AE (2010) The sigma-1 receptor is enriched in postsynaptic sites of C-terminals in mouse motoneurons. An anatomical and behavioral study. Neuroscience 167:247–255
Mavlyutov TA, Epstein ML, Liu P, Verbny YI, Ziskind-Conhaim L, Ruoho AE (2012) Development of the sigma-1 receptor in C-terminals of motoneurons and colocalization with the N, N′-dimethyltryptamine forming enzyme, indole-N-methyl transferase. Neuroscience 206:60–68
Meehan CF, Sukiasyan N, Zhang M, Nielsen JB, Hultborn H (2010) Intrinsic properties of mouse lumbar motoneurons revealed by intracellular recording in vivo. J Neurophysiol 103:2599–2610
Miles GB, Yohn DC, Wichterle H, Jessell TM, Rafuse VF, Brownstone RM (2004) Functional properties of motoneurons derived from mouse embryonic stem cells. J Neurosci 24:7848–7858
Miles G, Dai Y, Brownstone R (2005) Mechanisms underlying the early phase of spike frequency adaptation in mouse spinal motoneurones. J Physiol 566:519–532
Miles GB, Hartley R, Todd AJ, Brownstone RM (2007) Spinal cholinergic interneurons regulate the excitability of motoneurons during locomotion. Proc Natl Acad Sci 104:2448–2453
Milner-Brown H, Stein R, Yemm R (1973) The orderly recruitment of human motor units during voluntary isometric contractions. J Physiol 230:359–370
Misonou H, Mohapatra DP, Menegola M, Trimmer JS (2005a) Calcium-and metabolic state-dependent modulation of the voltage-dependent Kv2. 1 channel regulates neuronal excitability in response to ischemia. J Neurosci 25:11184–11193
Misonou H, Mohapatra DP, Trimmer JS (2005b) Kv2. 1: a voltage-gated k+ channel critical to dynamic control of neuronal excitability. Neurotoxicology 26:743–752

Mitra P, Brownstone RM (2012) An in vitro spinal cord slice preparation for recording from lumbar motoneurons of the adult mouse. J Neurophysiol 107:728–741

Mòdol-Caballero G, Santos D, Navarro X, Herrando-Grabulosa M (2018) Neuregulin 1 reduces motoneuron cell death and promotes neurite growth in an in vitro model of motoneuron degeneration. Front Cell Neurosci 11:431

Moreno CM, Dixon RE, Tajada S, Yuan C, Opitz-Araya X, Binder MD, Santana LF (2016) Ca2+ entry into neurons is facilitated by cooperative gating of clustered CaV1. 3 channels. Elife 5:e15744

Moritz AT, Newkirk G, Powers RK, Binder MD (2007) Facilitation of somatic calcium channels can evoke prolonged tail currents in rat hypoglossal motoneurons. J Neurophysiol 98:1042–1047

Mottram CJ, Suresh NL, Heckman C, Gorassini MA, Rymer WZ (2009) Origins of abnormal excitability in biceps brachii motoneurons of spastic-paretic stroke survivors. J Neurophysiol 102:2026–2038

Mottram CJ, Heckman CJ, Powers RK, Rymer WZ, Suresh NL (2014) Disturbances of motor unit rate modulation are prevalent in muscles of spastic-paretic stroke survivors. J Neurophysiol 111:2017–2028

Muceli S, Bergmeister KD, Hoffmann K-P, Aman M, Vukajlija I, Aszmann OC, Farina D (2018) Decoding motor neuron activity from epimysial thin-film electrode recordings following targeted muscle reinnervation. J Neural Eng 16:016010

Muennich EA, Fyffe RE (2004) Focal aggregation of voltage-gated, Kv2. 1 subunit-containing, potassium channels at synaptic sites in rat spinal motoneurones. J Physiol 554:673–685

Müller D, Cherukuri P, Henningfeld K, Poh CH, Wittler L, Grote P, Schlüter O, Schmidt J, Laborda J, Bauer SR (2014) Dlk1 promotes a fast motor neuron biophysical signature required for peak force execution. Science 343:1264–1266

Murakoshi H, Shi G, Scannevin RH, Trimmer JS (1997) Phosphorylation of the Kv2. 1 K+ channel alters voltage-dependent activation. Mol Pharmacol 52:821–828

Nagy J, Yamamoto T, Jordan L (1993) Evidence for the cholinergic nature of c-terminals associated with subsurface cisterns in α-motoneurons of rat. Synapse 15:17–32

Nascimento F, Broadhead MJ, Tetringa E, Tsape E, Zagoraiou L, Miles G (2020) Synaptic mechanisms underlying modulation of locomotor-related motoneuron output by premotor cholinergic interneurons. eLife 9:e54170

Negro F, Muceli S, Castronovo AM, Holobar A, Farina D (2016) Multi-channel intramuscular and surface EMG decomposition by convolutive blind source separation. J Neural Eng 13:026027

Nelson PG, Burke R (1967) Delayed depolarization in cat spinal motoneurons. Exp Neurol 17:16–26

Nelson P, Lux H (1970) Some electrical measurements of motoneuron parameters. Biophys J 10:55–73

Nordstrom MA, Gorman RB, Laouris Y, Spielmann JM, Stuart DG (2007) Does motoneuron adaptation contribute to muscle fatigue? Muscle Nerve 35:135–158

Pambo-Pambo A, Durand J, Gueritaud J-P (2009) Early excitability changes in lumbar motoneurons of transgenic SOD1G85R and SOD1G93A-low mice. J Neurophysiol 102:3627–3642

Pan Z, Kao T, Horvath Z, Lemos J, Sul J-Y, Cranstoun SD, Bennett V, Scherer SS, Cooper EC (2006) A common ankyrin-G-based mechanism retains KCNQ and NaV channels at electrically active domains of the axon. J Neurosci 26:2599–2613

Parmiggiani F, Stein R (1981) Nonlinear summation of contractions in cat muscles. II. Later facilitation and stiffness changes. J Gen Physiol 78:295–311

Perrier J-F, Hounsgaard J (2003) 5-HT2 receptors promote plateau potentials in turtle spinal motoneurons by facilitating an L-type calcium current. J Neurophysiol 89:954–959

Pinter M, Curtis R, Hosko M (1983) Voltage threshold and excitability among variously sized cat hindlimb motoneurons. J Neurophysiol 50:644–657

Piotrkiewicz M, Wilanowski G (2012) Is spike frequency adaptation an artefact? Insight from human studies. Front Cell Neurosci 6:50

Powers RK, Heckman CJ (2015) Contribution of intrinsic motoneuron properties to discharge hysteresis and its estimation based on paired motor unit recordings: a simulation study. J Neurophysiol 114:184–198
Powers RK, Sawczuk A, Musick JR, Binder MD (1999) Multiple mechanisms of spike-frequency adaptation in motoneurones. J Physiol Paris 93:101–114
Powers RK, Nardelli P, Cope TC (2008) Estimation of the contribution of intrinsic currents to motoneuron firing based on paired motoneuron discharge records in the decerebrate cat. J Neurophysiol 100:292–303
Rall W (1960) Membrane potential transients and membrane time constant of motoneurons. Exp Neurol 2:503–532
Rall W (1967) Distinguishing theoretical synaptic potentials computed for different soma-dendritic distributions of synaptic input. J Neurophysiol 30:1138–1168
Rall W (2011) Core conductor theory and cable properties of neurons. Compr Physiol:39–97
Revill AL, Fuglevand AJ (2017) Inhibition linearizes firing rate responses in human motor units: implications for the role of persistent inward currents. J Physiol 595:179–191
Romer SH, Deardorff AS, Fyffe RE (2019) A molecular rheostat: Kv2. 1 currents maintain or suppress repetitive firing in motoneurons. J Physiol 597:3769–3786
Sah P, Mclachlan EM (1992) Potassium currents contributing to action potential repolarization and the afterhyperpolarization in rat vagal motoneurons. J Neurophysiol 68:1834–1841
Sakmann B, Neher E (1984) Patch clamp techniques for studying ionic channels in excitable membranes. Annu Rev Physiol 46:455–472
Santiago LJ, Abrol R (2019) Understanding G protein selectivity of muscarinic acetylcholine receptors using computational methods. Int J Mol Sci 20:5290
Sawczuk A, Powers RK, Binder MD (1995) Spike frequency adaptation studied in hypoglossal motoneurons of the rat. J Neurophysiol 73:1799–1810
Schwindt PC (1973) Membrane-potential trajectories underlying motoneuron rhythmic firing at high rates. J Neurophysiol 36:434–439
Schwindt P, Crill WE (1977) A persistent negative resistance in cat lumbar motoneurons. Brain Res 120:173–178
Schwindt P, Crill W (1980a) Role of a persistent inward current in motoneuron bursting during spinal seizures. J Neurophysiol 43:1296–1318
Schwindt PC, Crill W (1980b) Effects of barium on cat spinal motoneurons studied by voltage clamp. J Neurophysiol 44:827–846
Schwindt PC, Crill WE (1980c) Properties of a persistent inward current in normal and TEA-injected motoneurons. J Neurophysiol 43:1700–1724
Schwindt PC, Crill WE (1981) Differential effects of TEA and cations on outward ionic currents of cat motoneurons. J Neurophysiol 46:1–16
Schwindt P, Crill W (1982) Factors influencing motoneuron rhythmic firing: results from a voltage-clamp study. J Neurophysiol 48:875–890
Smith CC, Brownstone RM (2020) Spinal motoneuron firing properties mature from rostral to caudal during postnatal development of the mouse. J Physiol 598:5467–5485
Soulard C, Salsac C, Mouzat K, Hilaire C, Roussel J, Mezghrani A, Lumbroso S, Raoul C, Scamps F (2020) Spinal Motoneuron TMEM16F acts at C-boutons to modulate motor resistance and contributes to ALS pathogenesis. Cell Rep 30(2581–2593):e7
Spielmann J, Laouris Y, Nordstrom M, Robinson G, Reinking R, Stuart D (1993) Adaptation of cat motoneurons to sustained and intermittent extracellular activation. J Physiol 464:75–120
Stecko GAJ (1962) A new bipolar electrode for electromyography. J Appl Physiol 17:849
Stein R, Parmiggiani F (1979) Optimal motor patterns for activating mammalian muscle. Brain Res 175:372–376
Stein R, French A, Mannard A, Yemm R (1972) New methods for analysing motor function in man and animals. Brain Res
Stifani N (2014) Motor neurons and the generation of spinal motor neurons diversity. Front Cell Neurosci 8:293

Takahashi T (1978) Intracellular recording from visually identified motoneurons in rat spinal cord slices. Proc R Soc Lond Ser B Biol Sci 202:417–421
Takahashi T, Berger AJ (1990) Direct excitation of rat spinal motoneurones by serotonin. J Physiol 423:63–76
Taylor JL, Amann M, Duchateau J, Meeusen R, Rice CL (2016) Neural contributions to muscle fatigue: from the brain to the muscle and back again. Med Sci Sports Exerc 48:2294
Thomas CK, Ross BH, Calancie B (1987) Human motor-unit recruitment during isometric contractions and repeated dynamic movements. J Neurophysiol 57:311–324
Thompson CK, Negro F, Johnson MD, Holmes MR, Mcpherson LM, Powers RK, Farina D, Heckman CJ (2018) Robust and accurate decoding of motoneuron behaviour and prediction of the resulting force output. J Physiol 596:2643–2659
Tsuchida T, Ensini M, Morton S, Baldassare M, Edlund T, Jessell T, Pfaff S (1994) Topographic organization of embryonic motor neurons defined by expression of LIM homeobox genes. Cell 79:957–970
Tsuzuki S, Yoshida S, Yamamoto T, Oka H (1995) Developmental changes in the electrophysiological properties of neonatal rat oculomotor neurons studied in vitro. Neurosci Res 23:389–397
Turkin VV, O'neilL D, Jung R, Iarkov A, Hamm TM (2010) Characteristics and organization of discharge properties in rat hindlimb motoneurons. J Neurophysiol 104:1549–1565
Ulfhake B, Cullheim S, Franson P (1988) Postnatal development of cat hind limb motoneurons. I: Changes in length, branching structure, and spatial distribution of dendrites of cat triceps surae motoneurons. J Comp Neurol 278:69–87
Umemiya M, Berger AJ (1994) Properties and function of low-and high-voltage-activated Ca2+ channels in hypoglossal motoneurons. J Neurosci 14:5652–5660
Veasey SC, Fornal C, Metzler C, Jacobs BL (1995) Response of serotonergic caudal raphe neurons in relation to specific motor activities in freely moving cats. J Neurosci 15:5346–5359
Viana F, Bayliss DA, Berger AJ (1993) Multiple potassium conductances and their role in action potential repolarization and repetitive firing behavior of neonatal rat hypoglossal motoneurons. J Neurophysiol 69:2150–2163
Vrbova G (1983) Hypothesis: Duchenne dystrophy viewed as a disturbance of nerve-muscle interactions. Muscle Nerve 6:671–675
Wachholder K (1928) Willkürliche Haltung und Bewegung, insbesondere im Lichte elektrophysiologischer Untersuchungen. Willkürliche Haltung und Bewegung, insbesondere im Lichte elektrophysiologischer Untersuchungen. Springer
Wienecke J, Zhang M, Hultborn H (2009) A prolongation of the postspike afterhyperpolarization following spike trains can partly explain the lower firing rates at derecruitment than those at recruitment. J Neurophysiol 102:3698–3710
Wilson JM, Rempel J, Brownstone RM (2004) Postnatal development of cholinergic synapses on mouse spinal motoneurons. J Comp Neurol 474:13–23
Yamada Y, Yamamura K, Inoue M (2005) Coordination of cranial motoneurons during mastication. Respir Physiol Neurobiol 147:177–189
Zagoraiou L, Akay T, Martin JF, Brownstone RM, Jessell TM, Miles GB (2009) A cluster of cholinergic premotor interneurons modulates mouse locomotor activity. Neuron 64:645–662
Zemankovics R, Káli S, Paulsen O, Freund TF, Hájos N (2010) Differences in subthreshold resonance of hippocampal pyramidal cells and interneurons: the role of h-current and passive membrane characteristics. J Physiol 588:2109–2132
Zengel JE, Reid SA, Sypert GW, Munson JB (1985) Membrane electrical properties and prediction of motor-unit type of medial gastrocnemius motoneurons in the cat. J Neurophysiol 53:1323–1344
Zhang L, Krnjević K (1987) Apamin depresses selectively the after-hyperpolarization of cat spinal motoneurons. Neurosci Lett 74:58–62
Zia M, Chung B, Sober SJ, Bakir MS (2018) Fabrication and characterization of 3D multi-electrode array on flexible substrate for in vivo EMG recording from expiratory muscle of songbird. In: 2018 IEEE international electron devices meeting (IEDM). IEEE, 29.4. 1–29.4. 4